Alma Mater Studiorum · University of Bologna

School of Science
Department of Physics and Astronomy
Master Degree in Physics

Advanced queuing traffic model for accurate congestion forecasting and management

Supervisor:
Prof. Armando Bazzani

Co-supervisor:
Dr. Filippo Dalla

Submitted by:
Gregorio Berselli

Academic Year 2023/2024

Abstract

Traffic congestion can be explained as a percolation in a dynamical system on a network structure because of the existence of a maximum flow rate, a finite transport capacity at crossing points and finite road capacity. In this thesis a mesoscopic traffic model is developed to study the congestion formation on a road network. The goal is to propose a predictive observable for the rise of congestion based on the traffic load fluctuations using the flow-density fundamental diagram of the network. The model simulates the vehicle dynamics using an average optimal velocity model along the road and introduces finite flow rates at the crossing points, also considering the traffic lights dynamics. Simulations are performed on a Manhattan-like network where all junctions are traffic lights or roundabouts. The main features of the congestion transition have been studied, both in stationary and transient states. A statistical analysis of traffic flow and density fluctuations was performed to highlight their predictive properties for congestion detection. From such simulations, flow fluctuations and normalized density fluctuations are highlighted to predict the rise of congestion when the system is in a stationary state. Furthermore, an optimization algorithm based on vehicle density is proposed and tested on a network consisting in traffic lights only. This algorithm shows good results regarding density fluctuations, which result lower with respect to unoptimized simulation for the same load. Despite that, the algorithm performs poorly on traffic flow, reducing it for the same load with respect to unoptimized simulations, mainly at high density. Thus, it appears unsuitable to manage congested systems. Finally, a test using data following a real trend is done on *Via Stalingrado* in Bologna, confirming the goodness of the model.

Contents

List of Figures

Introduction

The word *physics* has Greek origins and means *nature*. The aim to understand the nature of something implies a desire to comprehend the mechanisms governing the underlying system. But that's not the only way to interpret it. In modern age, the meaning of the word *physics* is more related to the field of study or the knowledge area, including all theoretical and experimental tools developed to understand any kind of phenomena. This second interpretation appears more interdisciplinary, extending the role of physics also in fields which are usually considered leaving in a "different world". The main example of an interdisciplinary field of physics is the *physics of complex systems*. Typically, complex systems are natural, social or dynamical systems which consist of many nonlinearly interacting elements [1]. These systems are constantly modifying their internal structure and patterns of activity in self-organization processes. The most important property of such systems is the existence of *emergent phenomena* which cannot be simply derived or predicted solely from the knowledge of the systems' structure and the interactions among their individual elements.

One example of complex systems are urban phenomena that constitute the "Physics of Cities", a new discipline which aims to understand cities from the complexity science perspective [2]. The study of cities as complex systems emerged in the second half of the 20th century [3]. In the last few years, the physics community has made a breakthrough in understanding such events with the help of an increasing quantity and quality of available data. Urban phenomena are indeed related to a wide class of studies, like study of racial residential segregation, empirical distribution of population density or income. Among all of them, there are also urban mobility phenomena. One example of application on mobility analysis can be the study of certain social dynamics. In principle social dynamics is not directly observable, but one can deduce some feature and characteristics by observing the human mobility: for example, a study in Venice highlighted some statistical correlation between bridges [4].

One of the most studied fields in city physics is road traffic. Traffic congestions are one of the most common problems for city development, which can decrease the quality of life, especially in urban areas, by increasing pollution [5]: in developing states of Asia, air quality of 97% of the cities is unhealthy [6]. Moreover, they can negatively affect the local regional economies [7]. With the rapid urbanization, socio-economic activities

tend to centralize only in few major cities in a country: this increases the number of the commuters daily traveling to the cities. But also, economy grows, leading to a household and vehicle population increase. By 2014, 54% of the world's population lived in cities (against the 30% estimated in the 1950s), and the United Nations predicts the urbanization level to grow up to 66% by 2050 [8]. Road traffic congestions also reduce productivity levels, costing time and energy: e.g. a 2011 study in the USA estimated a cost of $101 billion for American citizens.

A city can be seen as the overlap of many transport networks, i.e., cars, trains, buses, pedestrians, airplanes, and so on can be divided. However, every transport network can be stressed out, leading to many unwanted phenomena, e.g. traffic congestions. Everyday millions of drivers all over the world are on their way to work, holiday, airports and each of them knows for sure what a traffic jam is like. A traffic congestion usually occurs when the traffic demand is higher than the available network capacity, but it can also rise when the mobility demand is sustainable, in average. It is usually characterized by lower vehicle speed, increased travel times and longer vehicular queues. What have traffic congestions got to do with physics [9]? Over the years, many physical models were created and applied to network transportation problems [10]. The Lighthill-Whitham model (1955) [11], for example, was based on two premises: the conservation of the number of cars, which is indeed a rational assumption, and the existence of an equation of state describing a relationship between traffic flow and traffic density. The existence of an equation of state was partially verified by measurements, with much scatter observed in the data, particularly at high traffic densities. Nevertheless, this model provided a good representation of basic traffic phenomena like *shock waves* [12]. Another model, namely the Reuschel and Pipes model, described the movement of a car following another one in front assuming that the speed of the following car was a linear function of the distance between the lead car and the following car. During the 1970s, Herman and Prigogine (1979) put forward a *Two-fluid approach to town traffic* [13], which adapts the Boltzmann equation to vehicular traffic flows in a town, city or metropolitan area. Notice that there are many model types besides Lighthill-Whitham and gas kinetic ones, e.g. car following and cellular automata models [14].

Besides models for vehicular traffic, there are also models for bus-route systems, train and plane networks and pedestrian flow. In large metropolitan areas, the integration of different transport modes has become crucial to guarantee a fast and sustainable flow of people [15]. Using a network science approach, multimodal transport systems can be described as multilayer networks, where the networks associated to different transport modes are not considered in isolation, but as a set of interconnected layers. Moreover, many statistical physics tools were applied to traffic model, among which phase diagrams, linear stability analysis and density waves. The aim of such models is to unveil the nature of traffic flow and to optimize the transportation network itself to have an efficient society. In the last few years, their development has increased due to the diffusion of smart city concepts *Digital Twins*. A Digital Twin is a digital model

which serves as a counterpart of a real physical system, which aims to simulate its whole reality allowing to make better decisions. Cities are becoming smart not only in terms of the way we can automate routine functions serving individuals, buildings, traffic systems but in ways that enable monitoring, understanding, analyzing and planning the city to improve the efficiency, equity and quality of life for its citizens in real time [16]. However, most of those models are not used to prevent congestion because, to do it, many data are required to apply some multisource data fusion [17]. Indeed, traffic flows were the first data to be automatically sensed in cities and databases of various spatial data go back centuries [16]. However, these data are not free: installation and maintenance of the conventional detectors are expensive and induce serious disruption of traffic [18]. Moreover, collected data also need to be stored and analyzed: the analysis and mining of city traffic data plays a significant role in the optimization of public transport systems [8]. With some effort, large-scale experiments have shown how it is possible to find answers to many challenging analytical questions about mobility behavior, such as: What are the most popular itineraries followed by individual travels? What is the spatio-temporal distribution of such travels? How do people behave when approaching a key attractor, such as a stadium, station or airport? How can traffic jams and congestion be characterized and predicted?

The aim of this thesis project is to try to answer the last of these questions, with a focus on the congestion prediction. Considering the congestion as a collective effect of a dynamical complex system, statistical mechanics suggests that fluctuations should have a well-defined behavior near the critical point. Indeed, the intent of this work is to find any observable whose fluctuations could be predictive of the congestion formation. The work is divided in six chapters. The first chapter is a general overview of traffic models, in which also the main macroscopic observables like speed, density and flow are described. The second chapter contains a mathematical description of the framework used, with a focus on fluctuations and stochastic processes. The third chapter describes the model implementation, focusing on how every single component like a street, traffic light, roundabout, etc. has been schematized, together with sensors like magnetic loops, from a practical point of view. Then, two chapters are devoted to the analysis of data coming from numerical simulations. Chapter four contains the analysis of the system in a stationary state, where the number of agents in the network is slowly raised to simulate an adiabatic charging. This type of analysis permits an accurate study of fluctuations and the application of some algorithms, like peak-detection. Then, chapter five analyzes the system under an input based of some data loops collected by *Regione Emilia-Romagna* in the city of Bologna, including one simulation on *Via Stalingrado*. This analysis aims to more qualitative results with respect to the stationary one, testing the model behavior after some plausible inputs. Finally, the sixth chapter reviews the obtained results, discussing future developments and research topics which could start from this thesis.

Chapter 1

Traffic models

Traffic flow involves a multidimensional dynamical system of strongly interacting vehicles. For example, one can consider every car as an *elementary particle* constrained to move along a one-dimensional trajectory. Moreover, every car could obey to some other conditions: for example, it could have to go from a point A to a point B, without colliding with other particles. Traffic jams are the typical signature of the complex behavior of such system [10]. The aim is to use the concepts and the techniques of physics applied to such complex systems as transportation ones, making interdisciplinary research.

The first studies for traffic problems were done by Greenshields in 1935. Then, in 1955, Lighthill and Whitham came out with the oldest and most popular macroscopic dynamic model, based on the fluid-dynamic theory: they treated traffic as an effectively one-dimensional compressible fluid. In 1960, Prigogine proposed a gas-kinetic model based on the well-known Boltzmann equation. Newell, in 1961, developed the first optimal velocity model, a microscopic model based on the assumption of a delayed adaptation of velocity. During the '70s, Musha and Higuchi have studied the noisy behavior of traffic flow, conjecturing that the fluctuations of traffic current exhibit the so-called $\frac{1}{f}$ noise.

Nowadays, the development of traffic models is mainly done using computers and concepts of modern physics. It is now modelled as a system of interacting vehicles driven far from equilibrium, which shows a rich variety of physical phenomena such as dynamical jamming transitions, critical phenomena, metastability, self-organized criticality, nonlinear waves... A usual global approach is to represent the mobility demand by using an origin-destination matrix (possibly time dependent). The underlying assumption to the OD matrix existence is that individuals can be grouped into different communities that share the same spatial representation of the characterized city. These areas can be related to time-dependent socio-economic and cultural activities, like universities, hospitals and also commercial centers. Conversely, the origin areas are the residential or the suburbs areas where commuters live. Indeed, traffic dynamics is determined by distributing the individual mobility paths in the road network according to the individual OD demand. Is it possible to simulate the traffic dynamics by a random walk on a graph? If yes, what

is the error associated to such approximation?

Any model one wants to build must reproduce some common behaviors of traffic system. For example, it is well-known that vehicles move freely at low densities, while at high densities they are in a congested state. The phase transition between free and congested traffics shows also important behaviors such hysteresis and metastability. E.g., if the system is in a stationary state, it is possible to measure the probability to move from an area i to an area j. This probability is usually represented as the transition rate π_{ij}. To avoid congestion, traffic flows must be balanced, i.e.

$$\sum_j \pi_{ij} = \sum_j \pi_{ji} = d_i$$

meaning that the incoming degree is equal to the outgoing one. This condition makes the mobility evolve towards minimizing the congestion formation on the road network. From here it is also possible to write the average continuity equation

$$\dot{n}_i = \sum_j \pi_{ij}\phi\left(n_j\right) - d_i\phi\left(n_i\right)$$

where n_i is the population in the i area and ϕ is the vehicle flow. In a stationary situation, i.e. when $\sum_i n_i^\star = N$ constant, a solution $\phi_i^\star$ is the null eigenvector of the Laplacian matrix

$$L_{ij} = d_i\delta_{ij} - \pi_{ij}$$

From a statistical point of view, if the network is balanced then population fluctuations in a given area are well approximated by an exponential law

$$\rho\left(n\right) = \frac{1}{\bar{n}}e^{-\frac{n}{\bar{n}}}$$

with $\bar{n} = N/M$ and M the number of areas considered.

For what concerns traffic engineering area, many complex traffic models have been proposed: those models include so many factors that it is almost impossible to discover the essential factors affecting the traffic behavior. The goal of complex system physics is to simplify reality, i.e. making a model capable to reproduce the characterizing phenomena of a system using the smallest number of factors.

1.1 Relations among observables

The study of traffic phenomena mainly relies on few macroscopic observables: density, speed, flow (current) and travel times.

1.1.1 Density

In traffic theory, density is a key observable. It gives information about the number of vehicles located on a street. Moreover, during congestion, the density can also be used as indicator of the vehicle queue length at intersections. Let l be the length of a generic street and $n(t)$ be the number of vehicles on the street at time t. Then, the density $\rho(n, l, t)$ of a street can be defined as:

$$\rho(n, l, t) := \frac{n(t)}{l} \tag{1.1}$$

The density is usually expressed in vehicles per kilometer (veh/km) or kilometers to the minus one (km^{-1}).

1.1.2 Speed

Another important macroscopic observable is the speed of a vehicle, usually expressed in km/h (or m/s in simulations). Notice that this speed could also be a random variable. However, in a street network like a city one we have numerous vehicles, so usually the mean speed on each street is considered.

Let $\Sigma_v = \{1, \ldots, n_v\}$ be the collection of vehicles and let M be the total number of streets. Let's now take a natural number $m \leq M$ and let $S = \{s_1, \ldots, s_m\}$ be a partition of the vehicle set Σ_v. It is trivial that $\sum_i |s_i| = n_v$. Notice that a street can also be seen as an edge over a flat network. The mean speed over a street $s \in S$ can be written as:

$$\bar{v}_s := \mathbb{E}_s[v] := \sum_{i \in s} \frac{v_i}{|s|}$$

where v_i is the speed of the ith vehicle. Finally, the mean speed over an empty street is set to be v_0.

1.1.3 Flow

The mean flow over a street is defined as:

$$\phi := \rho v \tag{1.2}$$

Then, the flow is usually expressed in veh/h or h^{-1}.

However, this definition of the flow is hardly appliable in a real-world situation. An operative definition of the flow, used for data acquired by magnetic loop sensors, can be given as

$$\phi := \frac{\#\text{ vehicles passing on street } s \text{ in a time } \Delta t}{\Delta t} \tag{1.3}$$

1.1.4 Travel time

Among all observables, the one that is most used from everyone is surely the travel time. This is, in fact, the first information that many services like Google Maps [19] will return when asked for the best path to a given destination. By interpreting travel time as a disutility or burden, despite it is not easily reducible to an economic value, transport policy has been driven by the goal of quicker journeys [20].

The definition of travel time is straightforward: given a road network, and selected two nodes O (origin) and D (destination), the travel time Δt_{OD} is simply the time it takes to reach D from O. Notice that this definition is very general and shows how travel time does not depend on other observables.

1.1.5 Macroscopic Fundamental Diagrams

Macroscopic Fundamental Diagrams (MFDs) are graph relating average values of the main observable in a transport network, like the previous seen speed, flow and density. The most common diagram is the average flow - density one, used to evaluate traffic-control strategies [21]. A large urban network may have multiple flows for a given density, due to the presence of hysteresis loops.

However, if the traffic conditions are stationary, empirical data suggest that there must exist a relationship between flow, speed and density [22]. The first study on these relationships was done by Greenshields in 1935. A basic relation of traffic flow theory is indeed the Fundamental Traffic Formula, which is the flow definition from Eq. (1.2) and relates the three main observable of a traffic system. Usually, if traffic count data are available, then the traffic flow ϕ can be assumed as given as Eq. (1.3) and one can derive speed or density from the previous relation. Moreover, there are two special situations for a traffic system:

- When there are no cars at all, the density is zero and so the flow. In this condition the speed behaves much as a theoretical value, and it is standard to assume it as the speed limit v_0;
- When the density exceeds the so-called *jam density* threshold ρ_c, speed and flow are both zero and all movement stop. For a simulation this is not an optimal situation because it can lead to permanent locks, and this is why one usually set the minimum possible value of speed to be non-zero.

Between these extreme points, while density increases the flow does the same, despite the speed going down due to vehicle interactions. One can clearly see this effect in Fig. 1.1.

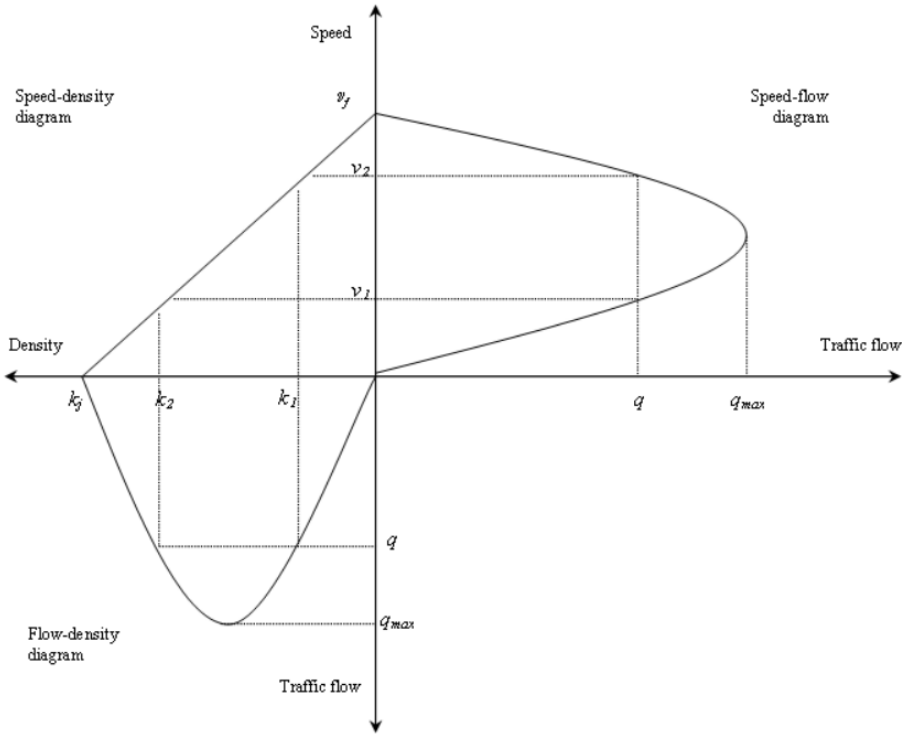

Figure 1.1: *Macroscopic Fundamental Diagrams relating speed (v), density (k) and flow (q) [22].*

1.2 Queuing models

In the literature, it has been shown that queuing models can be used to adequately model uninterrupted traffic flows [22]. Congestion depends on many factors, e.g. the number of vehicles on the road, therefore it is necessary to build models which can capture any of them. Notice that traffic flows are usually modelled empirically, starting from collected speed and flow data: this approach is limited in terms of predictive power and sensitivity analysis. One alternative to this can be analytical models based on queuing theory: here vehicles are going to spend time in a network influenced by queues.

We can divide traffic flows in two main groups:

- *uninterrupted flows*, where flow is regulated through vehicle-vehicle and vehicle-roadway interactions;
- *interrupted flows*, where flow is regulated by an external signal. Vehicle-vehicle and vehicle-roadway interactions are also present but, in this case, they play a secondary role.

Once the type of flow is defined, the next step consists of model selection. In the next subsections the three main macro areas in which all models can fall are described: microscopic, mesoscopic and macroscopic models. Notice that microscopic and mesoscopic models are typically more complex and not analytically solvable, making them demand a lot of computer time. Therefore, macroscopic models are better mathematical tools due to their analytical description while other models are more like simulation tools.

Microscopic models

Microscopic models describe a traffic system with an elevated level of detail. Each vehicle is typically represented separately and models are based on theories about vehicle maneuvers through traffic. These models are thought for:

- *car-following theories*, in which each vehicle acts based on the vehicle in front of it;
- *time-space diagrams*, commonly used to solve transportation-related problems;
- *microsimulations*, such software solutions like SUMO [23].

Macroscopic models

On the other hand, macroscopic models describe a traffic system with low level of detail, usually by aggregating all vehicles in flows. One can use this type of models for:

- *capacity analysis*, like level-of-service analysis for highways;
- *MFDs*, to study speed-flow-density relationships;
- *shock wave analysis*, because a shock wave exists whenever the traffic condition changes.

Mesoscopic models

Lastly, one can have a mix between microscopic and macroscopic models, the so-called mesoscopic models. In this model the traffic system is represented with high level of detail, thus describing interaction with low detail level. These models can be categorized into:

- *headway distribution models*, describing the distribution of headways, i.e. the passage times difference of two successive vehicles, while neither explicitly considering each vehicle separately;
- *cluster models*, studying group of vehicles which shares a specific property and treating them like a single entity over the system;

- *gas-kinetic continuum models*, describing velocity distributions and able to reproduce some non-linear dynamics.

In queuing models, traffic flow is usually assumed stationary (*steady-state queuing models*) and all vehicles will always be moving with non-zero speed, no matter how slow. Moreover, non-stationary traffic can be studied, e.g. stop's ang go's phenomena, using so-called *transient queuing models*.

1.3 Open Traffic Models

The state of the art as traffic simulation platform is the *Open Traffic Models* (OTM) *framework* [24]. OTM is a framework which allows any user to run a variety of models such as queuing ones but also car-following and fluid-based models. So, using this framework one can simulate on all microscopic, mesoscopic and macroscopic models. This approach works with two main components:

1. A network description which is a bridge between single pipe graphs typical of macroscopic models and the lane-by-lane representation of microscopic models. All lanes in each lane group are assumed to be synchronized in speed forming a sort of "longitudinal dynamics". This approach corresponds to a single lane of vehicles in microscopic models, a queue pair in mesoscopic models and a differential equation for a macroscopic model.

2. Since every link can be modeled with a different nature, a protocol has been implemented to coordinate models, i.e. to manage the passage of flow packages from one link to another. This protocol was inspired by the Godunov scheme for partial differential equations.

Moreover, the framework also implements sensors and actuators to acquire data for simulations. Finally, OTM is fully open-source and supports the implementation of third-part models as plugins.

Chapter 2

Stochastic traffic model on a road network

The basis of a traffic flow simulation is certainly a road network. For the sake of the analyses, a planar network is considered, i.e. a graph which can be drawn on two-dimensional such that no edges cross each other. Let's call N the number of nodes in the graph and M the number of edges. The edge density is then defined as

$$C := \frac{M}{N}$$

From now on, the edges will be addressed as *streets* and the nodes will be addressed as *junctions*.

2.1 Street dynamics

The state of a network road is given by its density, as defined in Eq. (1.1). To simplify the model, the input velocity on a road will be assumed to be a function of such density:

$$v(\rho) = v_0 \left(1 - \alpha \frac{\rho}{\rho_{\max}}\right) \tag{2.1}$$

where v_0 represents the free velocity (i.e. the road speed limit), $\alpha \in]0, 1]$ is a parameter used to keep $v \in [v_{\min} \geq 0, v_0]$ and $\rho_{\max}$ is the maximal road density. A plot for different values of α and fixed $v_0 = 13.9\ m/s$ (corresponding to 50 km/h) is reported in Fig. 2.1.

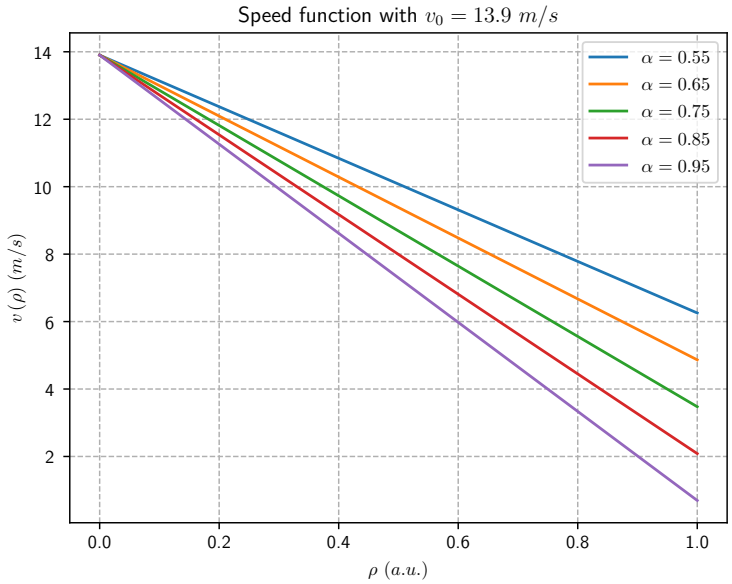

Figure 2.1: *Plot of the speed function of Eq. (2.1) for* $\alpha \in \{0.55, 0.65, 0.75, 0.85, 0.95\}$. *For the sake of simplicity, the density has been scaled as* $\rho \to \rho/\rho_{max}$.

Consequently, using Eq. (1.2) the flow of the street becomes

$$\phi(\rho) = \begin{cases} \rho v_0 \left(1 - \alpha \frac{\rho}{\rho_{\max}}\right) & , \quad \rho \leq \beta \rho_{\max} \\ \beta v_0 \left(1 - \alpha \frac{\beta}{\rho_{\max}}\right) & , \quad \text{otherwise} \end{cases} \tag{2.2}$$

where $\beta \in \left[\frac{1}{2\alpha}, 1\right]$ defines the average traffic flow during congested states [25]. By doing a simple derivative one can find the critical density ρ_c, i.e. the density for which flow has a local maximum:

$$\rho_c = \frac{\rho_{\max}}{2\alpha} \tag{2.3}$$

It is trivial that, normalizing $\rho_{\max} = 1$, $\rho_c > \frac{1}{2}$. In this case, $\rho_c \geq 1$ for $\alpha \leq \frac{1}{2}$ and the parameter makes, in this case, the system loses some physical meaning. Therefore, one should limit $\alpha \in \left]\frac{1}{2}, 1\right]$. A plot for different values of α and $\beta = \frac{2\alpha+1}{4\alpha}$ is reported in Fig 2.2.

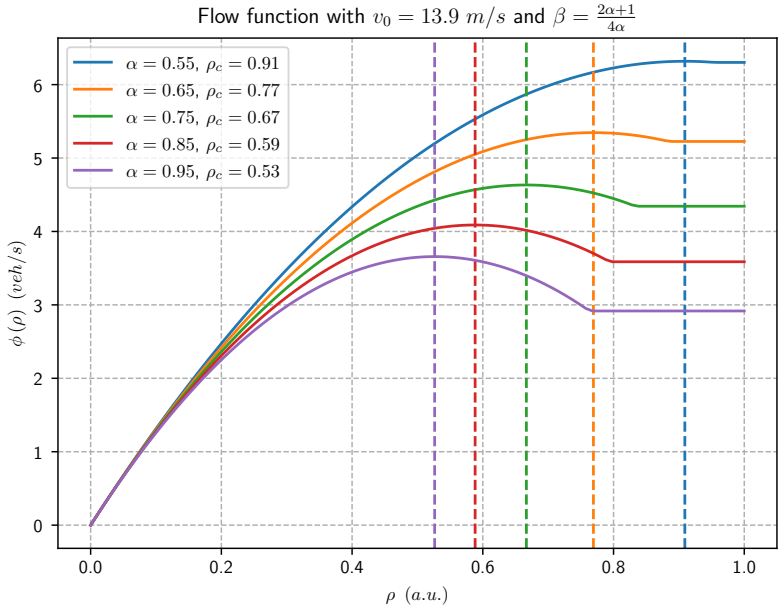

Figure 2.2: *Plot of the flow function of Eq. (2.2) for* $\alpha \in \{0.55, 0.65, 0.75, 0.85, 0.95\}$. *Dashed lines are at the points of maximum. The parameter* β *is always considered to be* $\frac{2\alpha+1}{4\alpha}$. *For the sake of simplicity, the density has been scaled as* $\rho \to \rho/\rho_{max}$.

At this point it is convenient to scale the density $\rho \to \rho/\rho_{\max}$, the time $t \to tv_0/l$ and the flow $\phi \to l\phi/v_0$. From now on, all symbols will refer to scaled variables.

The normalized density-flow relationship is then

$$\phi\left(\rho\right) = \begin{cases} \rho\left(1-\alpha\rho\right) & , \quad \rho \leq \beta \\ \beta\left(1-\alpha\beta\right) & , \quad \text{otherwise} \end{cases}$$

The maximal flow value at critical density can be written as

$$\phi_{\max} = \rho_c\left(1-\alpha\rho_c\right)$$

This means that it exists a stable solution ρ^{eq} to the equation

$$\rho^{\text{eq}}\left(1-\alpha\rho^{\text{eq}}\right) = \phi_{\text{in}}, \quad \phi_{\text{in}} \leq \phi_{\max}$$

Notice that the input flow depends on the output flow of incoming roads, so one can write the road dynamics as

$$\dot{\rho} = -\phi\left(\rho\right) + \phi_{\text{in}}\left(t\right) \tag{2.4}$$

2.1.1 Density fluctuations effects

Before jumping into junction dynamics, let's study the effect that density fluctuations have on a road flow. Starting from Eq. (1.2), one can write:

$$\begin{aligned}\phi(\rho+d\rho) &= (\rho+d\rho)(1-\alpha(\rho+d\rho)) \\ &= \rho(1-\alpha\rho) - \alpha\rho d\rho + d\rho(1-\alpha(\rho+d\rho)) \\ &= \phi(\rho) + d\rho(1-2\alpha\rho) - \alpha d\rho^2\end{aligned}$$

thus,

$$\Delta\phi = \phi(\rho+d\rho) - \phi(\rho) = d\rho(1-2\alpha(\rho+d\rho))$$

Notice that by decreasing fluctuations, i.e. $d\rho < 0$, one has that the flow increases if and only if $\rho + d\rho > \frac{1}{2\alpha} \equiv \rho_c$.

2.2 Junction dynamics

To describe the dynamics over the whole network, Eq. (2.4) has to take into account also the dynamics at crossing points. Let's introduce a stochastic matrix $\pi_{ij}(t)$ which defines the probability that the outgoing flow from the ith street enters the jth one. The time dependence of such matrix simulates the flow fluctuations at junctions. Moreover, assume that it is symmetric and

$$\sum_i \pi_{ij}(t) = 1$$

To simplify the problem, the network will be assumed as homogeneous, to have the same scaling variables. At this point one can write the network dynamics starting from the road's one

$$\begin{aligned}\dot{\rho}_i(t) = &-\sum_i \pi_{ij}(t)\,\rho_i(t)\,(1-\rho_i(t)) \\ &+\sum_i \pi_{ji}(t)\,\rho_j(t)\,(1-\rho_j(t))\end{aligned} \tag{2.5}$$

Notice that, in absence of external vehicle sources, Eq. (2.5) is conservative

$$\sum_i \dot{\rho}_i(t) = 0$$

then there exists an integral of motion $\sum_i \rho_i(t) = C \leq \beta M$ which expresses the conservation of the total vehicle number.

2.2.1 Classic junction

As result of previous assumptions, one can split the stochastic matrix in an average and a linearly independent fluctuating part

$$\pi_{ij}(t) = \pi_{ij}^{0} + \xi_{ij}(t)$$

with $\xi_{ij}(t) : \mathbb{E}[\xi] = 0, \sum_j \xi_{ij}(t) = 0$. For physical reasons, one should also constrain the fluctuations in such a way that $0 \leq \pi_{ij}(t) \leq 1$. The covariance matrix can be written as

$$\mathbb{E}\left[\xi_{ij}(t)\,\xi_{i'j'}(t')\right] = c_{\tau_c}\left(|t-t'|\right)\delta_{ii'}\sigma_{i,jj'}$$

where τ_c is the correlation time, the factor $\delta_{ii'}$ expresses independence of different streets and $\mathbb{E}\left[\xi_{ij}\sum_{j'}\xi_{i'j'}\right] = \sum_j \sigma_{i,jj'} = 0$.

At this point, the equilibrium states $\rho^{\mathrm{eq}} < \rho_c$ must satisfy the constraint

$$\sum_i \pi_{ij}^{0}\phi_i^{\mathrm{eq}} - \sum_i \pi_{ji}^{0}\phi_j^{\mathrm{eq}} = 0$$

where the equilibrium flow is defined as

$$\phi_i^{\mathrm{eq}} = \rho_i^{\mathrm{eq}}\left(1 - \alpha\rho_i^{\mathrm{eq}}\right)$$

Notice that one can simplify the previous relationship

$$\sum_i \left(\pi_{ij}^{0} - \delta_{ij}\right)\phi_i^{\mathrm{eq}} = 0 \tag{2.6}$$

thus, the equilibrium solution is given by $a\phi_i^{\mathrm{eq}} = \phi\left(\rho_j^{\mathrm{eq}}\right)$ with $\sum_i \rho_i^{\mathrm{eq}}\left(\phi_i^{\mathrm{eq}}, a\right) = C$ where a measures the total traffic flow on the whole network. The solution for non-congested equilibrium of Eq. (2.6) is achieved for

$$a\phi_i^{\mathrm{eq}} < \phi_{\max} = \frac{1}{4\alpha}$$

The parameter C, which represents the average density, is a control parameter.

Chapter 3

Model implementation

The actual implementation of the model follows the path set by a previous work [26]. Starting from an existing model, many features are added in order to make more detailed simulations [27]. Due to computational necessities, this implementation is discrete-timed. Thus, every execution of the evolution algorithm (described in Section 3.4) corresponds to one time step which it was decided to match with a second.

3.1 Streets

The main rework for what concerns streets is the addition of queues. Streets are implemented with two buffers: one buffer for the vehicles circulating in the street and one exit queue which orders vehicles leaving the street. Each vehicle which enters the street goes in the first buffer with a speed $v = v(\rho)$ as set by Eq. (2.1): it will be assigned a penalty time $t = l/v$, rounded to the closest integer greater than t, during which it has to stay in the initial buffer. Once served the penalty, the vehicle will move on the exit queue, and it is assigned a null speed. From here, one agent for time unit is free to leave the exit queue and enter the next junction. Notice that queues are FIFO structures, which stand for *first in, first out*. Thus, at each time step, the agent who will leave the queue is the one who has been there the longest.

Finally, one can also set up the equivalent of magnetic loops on streets, to count the vehicle passing in a given time. These loops can be placed in both input, counting every agent as it is placed on the street, and output, counting every agent as it moves away from the street.

3.1.1 Mean speed optimization

Starting from Eq. (2.1) one can rewrite the input speed formula as

$$v\left(n\right) = v_0 \left(1 - \alpha \frac{n}{n_{\max}}\right)$$

where n is the number of vehicles on the street and $n_{\max}$ is the maximum number of vehicles the street can hold. Assuming that the street queue is empty, i.e. there are no vehicles waiting at a junction, meaning all vehicles are moving, it is possible to compute the mean speed over the street without cycling through the agents

$$\bar{v}\left(n-1\right) = \frac{1}{n}\sum_{k=0}^{n} v_0 \left(1 - \alpha \frac{k}{n_{\max}}\right) = v_0 \left(1 - \frac{\alpha\left(n-1\right)}{2}\right)$$

thus obtaining better computational performances. Notice that this method is valid only for moving vehicles and in a different case it is necessary to make a weighted average between this formula and all waiting agents.

3.2 Junctions

Many types of junctions are actually implemented. All of them have a vehicle buffer, which is managed differently accordingly to the junction type, and a pair of coordinates. Notice that at every time step all junctions try to empty their buffer, regardless of their type. Moreover, most junctions have a priority system to simulate real-life road junction. To make an example on how this algorithm works, consider a simple junction like the one represented in Fig. 3.2.

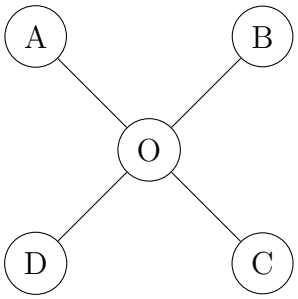

Figure 3.1: *Simple road intersection with five nodes and four streets. Nodes have coordinates* $O = (0, 0)$*,* $A = (-1, 1)$*,* $B = (1, 1)$*,* $C = (1, -1)$ *and* $D = (-1, -1)$*.*

Assuming to know the coordinates of each node one is able to compute the difference in direction due to turns. Let's define a score function which depends on the direction

change $\Delta\theta = \theta_{\text{out}} - \theta_{\text{in}}$:

$$s\left(\Delta\theta\right) := \frac{\Delta\theta}{2\pi} - f\left(\Delta\theta\right) + \frac{1}{2} \tag{3.1}$$

with:

$$f\left(x\right) = \begin{cases} \text{sign}(x) & , \quad |x| > \pi \\ 0 & , \quad \text{otherwise} \end{cases}$$

The vehicle with the highest priority is the one with the lowest value of the score in Eq. (3.1). Moreover, as one can see in Fig. 3.2, the score function is normalized $s\left(\Delta\theta\right) \in [0, 1] \quad \forall \Delta\theta \in [-2\pi, 2\pi]$.

So, suppose there are three vehicles, both going to C but coming from A, B and D. Then, one has that $\Delta\theta_{AC} = 0$, $\Delta\theta_{BC} = \pi/2$ and $\Delta\theta_{DC} = 3\pi/2$ so $s\left(\Delta\theta_{AC}\right) = 0$, $s\left(\Delta\theta_{BC}\right) = \pi/2$ and $s\left(\Delta\theta_{DC}\right) = -\pi/2$. Finally, the vehicle coming from D will pass first (right turn), then will pass the one coming from A (straight turn) and lastly will pass the one coming from B (left turn). Notice that one can adapt this algorithm to left-turn priority systems (like the Great Britain one) by transforming $\Delta\theta \to -\Delta\theta$.

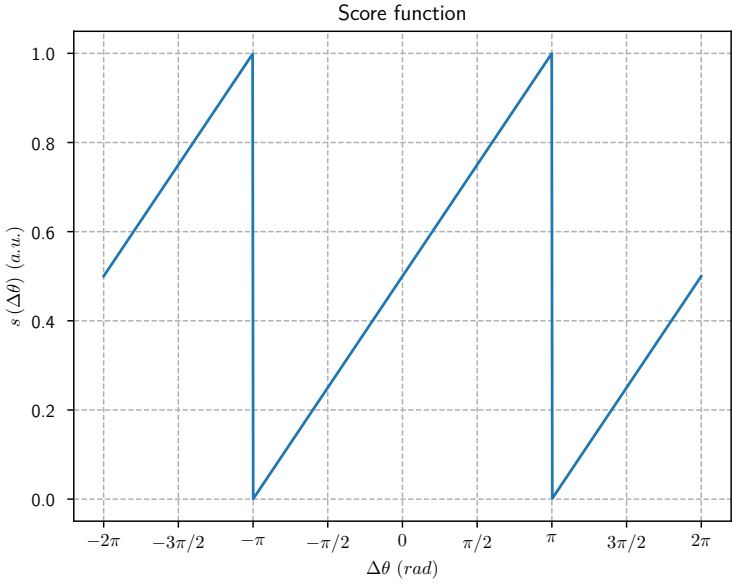

Figure 3.2: *Plot of the score function for* $\Delta\theta \in [-2\pi, 2\pi]$.

3.2.1 Traffic Lights

A traffic light is a type of node that accepts input vehicles only from part of the roads connected to it and blocking it in the remaining ones. After a defined time period, the blocked roads are unlocked and vice versa. Vehicles that are allowed to pass through are

still subject to the precedence rules of normal intersections. It has been implemented with a pair of delays (g, r), namely containing the *green* and *red* light timings expressed in discrete time units of the simulation. Suppose to have a junction like the previous one seen in Fig. 3.2 and suppose to have a traffic light node as node O. Moreover, let's assume that this semaphore will prioritize straight connections (i.e. A-C and B-D) and the green-red cycle is referred to the A-C link. At this point, the node will allow the vehicles to flow between A and C for g time steps between B and D for r time steps. Notice that the semaphore timings are not symmetrical a priori, i.e. one link could allow vehicles to flow for a longer time with respect to the other link.

3.2.2 Roundabouts

Roundabouts junction are slightly different from nodes seen above. They implement the vehicle buffer as a queue. Thus, the FIFO structure of queues introduces an intrinsic precedence system and so roundabouts are not relying on Eq. (3.1). In addition, to keep the implementation realistic, a decision was made to forbid U-turns in all non-roundabout junctions.

3.3 Vehicles

The implementation of vehicles is meant to consider all of them equal. Therefore, this model will not distinguish between a bus, an SUV, a truck, or a subcompact car as they all will be treated as point-like particles. Physical space management is left to the streets. The only parameter required to build a vehicle is its path. Then, the code will manage by its own the vehicle's position (node or street), the time penalty it has to wait, its speed and travelled time and distance.

3.4 Dynamics

The dynamics of the system is given by the evolution algorithm, which consists of three main parts: firstly, agents are moved from streets into junctions (if possible), then they are moved from every junction to the next streets (if possible) and, lastly, every agent is either updated or inserted for the first time in the system. It was decided to implement the algorithm in this way since it does not require copying entire data structures, making the execution lighter.

In detail, the three stages of the algorithm are:

1. *Street evolution*: for each street, the agent in front of the exit queue is taken (if present). Then, if the destination node has at least one free spot for it, it is moved from the street's queue into the node buffer, otherwise it stays on the street. If the

destination node is the journey destination of the agent, it will be removed from the system;

2. *Junction evolution*: for each node, a cycle over the agents on it is made in order to pull out as many agents as possible. In particular, for each agent the next street is computed (basing on Dijkstra's algorithm [28]): if the street has at least one free slot, the agent will be moved from the junction to the street, updating its speed and delay time. If it cannot move, there are two possible cases: if the node is a roundabout, other agents will be skipped, otherwise the algorithm will try to move other agents;

3. *Agent evolution*: for each agent with an assigned node/street, the travel time and the delay are respectively increased and decreased (this last if greater than zero) by one unit. If the agent has no node nor street assigned, it will be put in the system either randomly or precisely, depending on the user input.

At the end of all, also the simulation time is increased by one.

Chapter 4

Simulation results in stationary conditions

For research purposes, the first numerical simulations are done with the system in a quasi-stationary state. Stationary systems are usually considered for correlation and autocorrelation studies and because they could be required by some algorithms, like peak detection ones. The aim of simulations in this chapter is indeed to approximate an adiabatic charge of the dynamical system studied, in such a way to study the fluctuations of the main observables. Adiabatic charge means that the network is constantly loaded while trying to keep the mean density almost constant.

All the simulations are performed on a Manhattan-like road network, consisting in 120 nodes and 436 streets, as represented in Fig. 4. Every street is 2 km long and has a maximum capacity of 225 vehicles. Consequently, the maximum vehicle density corresponds to 112.5 veh/km. The speed limit is also common to all of them, and it's set to 50 km/h. To acquire the greatest amount of data, we associate a loop to each road, which counts the transiting vehicles during a given timespan. In particular, a street counter is increased by one whenever a vehicle leaves that street. Moreover, each street has 1 as transport capacity, meaning that it is able to move at most one vehicle per unit time, which in this case corresponds to 1 s. On the other hand, every node, independently on its nature, has a transport capacity equal to the input degree, meaning that in an ideal situation it is able to move every vehicle coming from its connected streets.

For what concerns the control parameters of the model, $\alpha = 0.95$ with an error probability of 5%. Notice that the error probability represents the probability that in a time step a vehicle would act like a random vehicle: it might still follow the shorter path.

Moreover, every simulation has the following characteristics:

- All vehicles inserted spawn with an assigned random path on a random network

street;

- All and only the border nodes are considered like exits.

For example, a vehicle could spawn on the street $33 \to 45$, having to go to node 96.

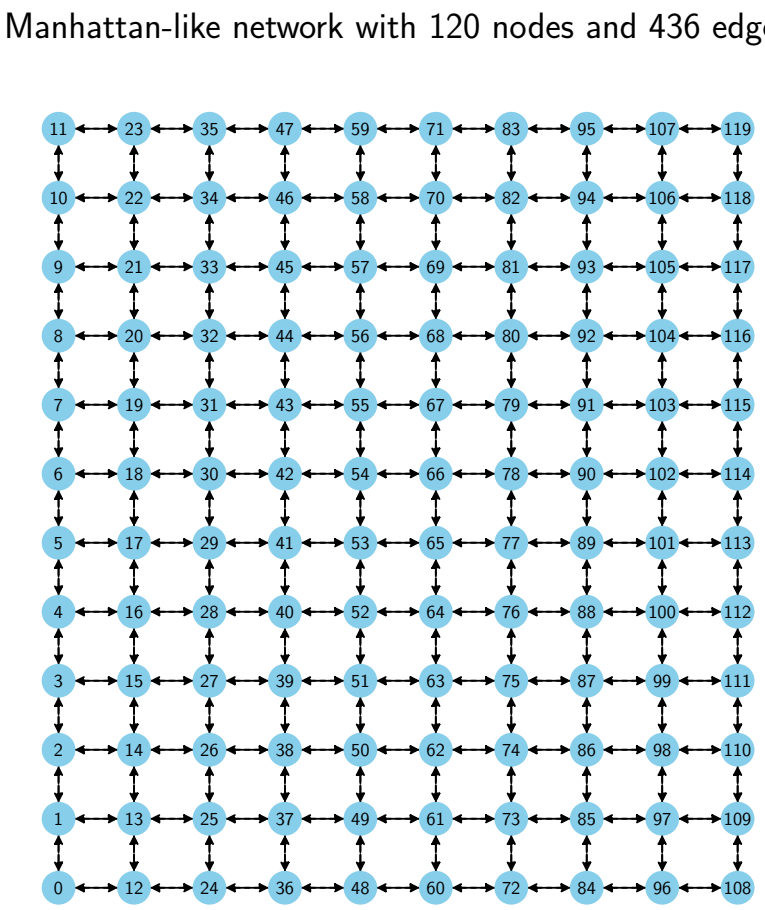

Figure 4.1: *10x12 Manhattan-like network with 120 nodes and 436 edges.*

In this case of steady simulations, vehicles are added once a minute but smoothly over time. Every simulation starts adding 450 vehicles per minute uniformly over all

the road network. Then, if the difference of the total number of vehicles over the net is negative over forty minutes, the number of added agents is increased by one. This process is repeated until the simulations stops, having the maximum number of agents on every street. The simulation is interrupted once the maximum density is reached.

Finally, the flow that will be considered is the operative one defined in Eq. (1.3) and retrieved by the loops put on the streets.

In this chapter, the predictive quality of both flow and density fluctuations emerges in Sec. 4.1 for traffic lights and Sec. 4.2 for roundabouts. Then, an optimization algorithm discussed in Sec. 4.1.1 shows reliable results in lowering densities fluctuations, cooling the system, but poorly performs for what concerns traffic flow, decreasing it with respect to the load compared with unoptimized simulations.

4.1 Traffic Lights

As first study case let's consider the system when all the 120 junctions are traffic lights. In this case, one has two more control parameters per node, for a total of 240. These parameters are the green and red time of each traffic light, as previously described in Sec. 3.2.1. To have a uniform dynamics over the system, they are set to be randomly assigned by sampling from a normal distribution with mean $\mu = 60\ s$ and standard deviation $\sigma = 10\ s$. Notice that is not required that all traffic light have the same cycle duration, but they all have green time equal to red time. For all the analyses performed in this section, data points are taken every five minutes. As before, let's comment the fundamental diagram first.

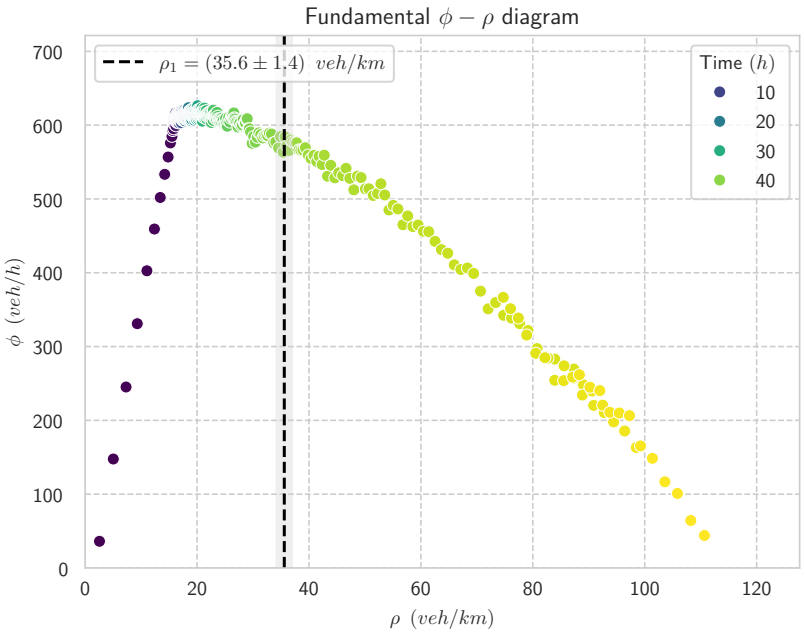

Figure 4.2: *Fundamental flow/density diagram for a stationary simulation on a network composed by traffic lights.* ρ_1 *corresponds to the density at which the formation of the Giant Component occurs, at time* (40.8 ± 0.9) h*. The plot is the resulting average of five different simulations which have all the same parameters but the seed.*

In Fig. 4.1 is drawn the fundamental flow/density diagram for a simulation containing traffic lights only. Here one can see that at low densities, the flow/density relationship is linear: this is expected as from the flow definition in Eq. (1.2). Then, as hypothesized in Eq. (2.2), a plateau is reached around 20 veh/km density, and one has a nearly constant flow for many density values. This is actually a problem from a practical point of view. Let's suppose to have a real road network and to put some magnetic loops on it in such a way to gather the number of vehicle passages in a given timespan. With only this data, it seems that one cannot tell exactly where the system is on the load curve. Thus, it could be very hard to predict the congestion formation. Returning to the chart analysis, after the plateau the congestion occurs, causing the flow to decrease while the density increases. Finally, there is no sign of hysteresis cycles in the plot, due to the fat that the network is constantly loaded, never letting it discharge.

The goal of this simulation is to find any observable which works as congestion forecaster. Firstly, one needs to define what a congestion is. Considering the whole network, every street has a vehicle density which in this case is limited $\rho \in [0, 112.5]$ veh/km.

The congestion state of any street will be defined by the following threshold function

$$\theta_\rho := \theta(\rho - \rho_c) \tag{4.1}$$

where ρ_c is the critical density defined in Eq. (2.3) and θ is the Heaviside step-function. At this point, the congestion time will be defined as the creation of the Giant Component composed of congested streets. In other words, given the Giant Component size over the density, the bigger step between consecutive points corresponds to the congestion formation. In order to find this, an algorithm has been implemented to create a network composed only by streets with $\theta_\rho = 1$ for each time step, computing every time the Giant Component size.

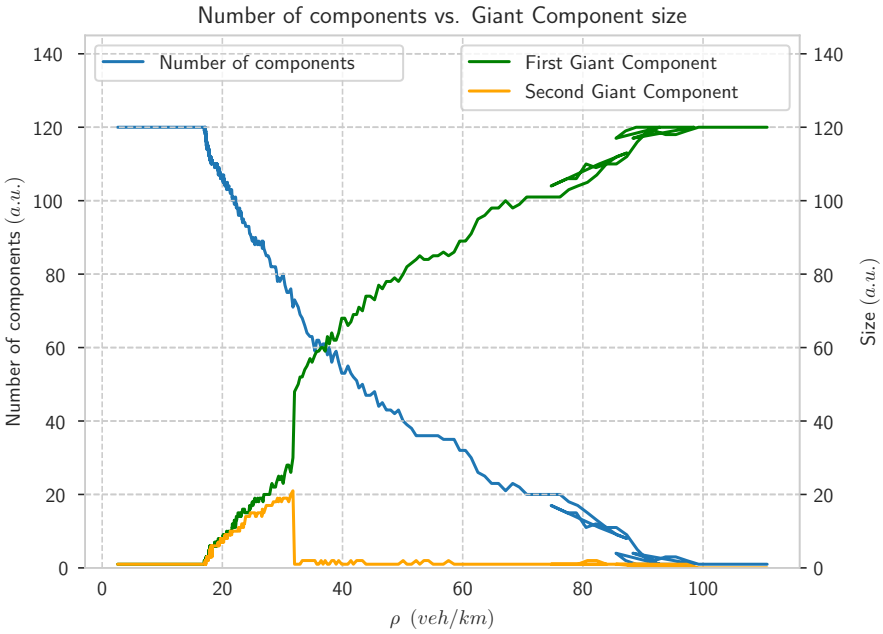

Figure 4.3: *Number of components with $\theta_\rho = 1$ versus the first and second component sizes. The Giant Component formation occurs when the bigger delta size of both first and second component appears, meaning that they have joined one into the other. The plot is the resulting average of five different simulations which have all the same parameters but the seed.*

In Fig. 4.1 one can see the trend of the Giant Component size over the mean density. The bigger delta is located at $\rho_1 = (35.6 \pm 1.4)\ veh/km$.

To search for a congestion forecaster, and assuming to have only loops data available, let's look at the flow fluctuations compared with the mean network density. The flow fluctuations are computed as follows: for every timespan, i.e. every five minutes, the

mean flow over all streets is computed starting from the loops' measurement. Then, fluctuations of a variable x at a given time are computed using the following formula:

$$\sigma_\phi := \sqrt{\frac{\sum_{i=0}^{M} \left(\phi_i - \bar{\phi}\right)^2}{M-1}} \tag{4.2}$$

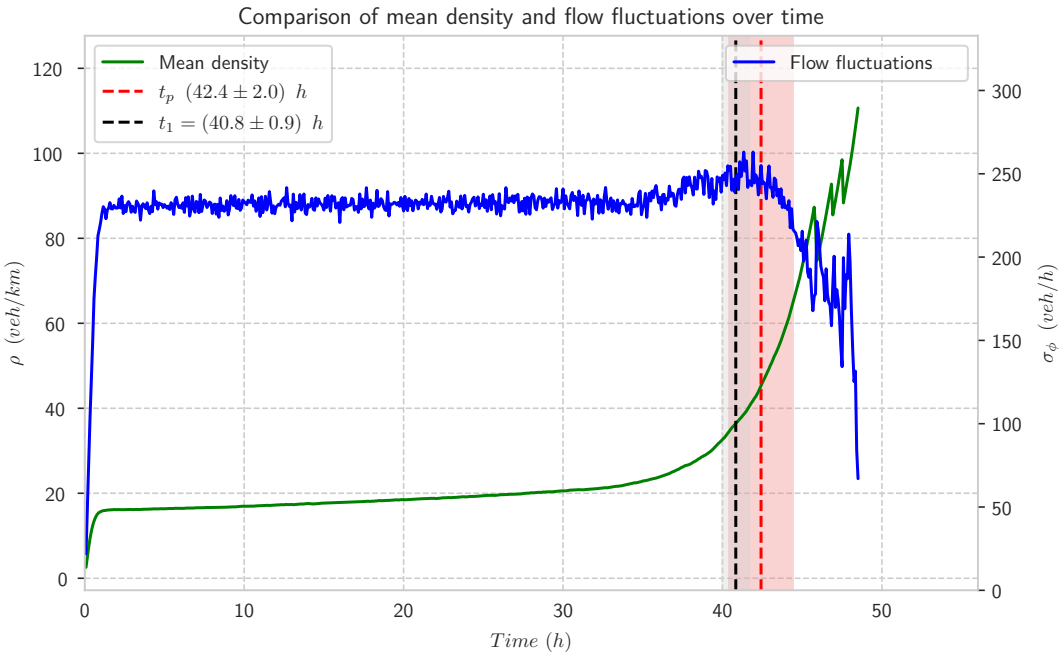

Figure 4.4: *Time plot of mean network density vs mean flow fluctuations. The parameters used for the peak detection algorithm are $l = 500$, $t = 5$ and $i = 0$. t_1 corresponds to the time at which the formation of the Giant Component occurs. t_p corresponds to the time at which the peak is detected. The plot is the resulting average of five different simulations which have all the same parameters but the seed.*

The flow fluctuations computed using Eq. (4.2) are compared with the mean density in Fig. 4.1. Notice that density, as well as fluctuations, remains almost constant over time, meaning that the system is in a stationary state. Due to the continuous charging, there's a time in which the network cannot hold the mobility demand, making also the mean density explode. In fact, from this time on, mean density increases until it reaches it maximum value, recalled being 112.5 veh/km. During this phase the traffic system naturally passes through a phase transition from free to congested state. One can notice this by looking at the flow fluctuations, which amplify as the density begin to increase.

By using a peak detection algorithm [29] (more details in Appendix A) one can clearly highlight the first peak of the fluctuations, in this case at a time of (42.4 ± 2.0) h. Notice that this time is perfectly compatible with the formation time of the Giant Component, which is (40.8 ± 0.9) h. Thus, flow fluctuations may be a good forecaster for traffic congestions.

Let's now have another look to Fig. 4.1: the critical density appears to be slightly more than 20 veh/km. This fact is strange for at least two reasons. Firstly, the maximum capacity of each street, as the parameters were set, is of 112.5 veh/km and this means that the observed critical density is less than the 20% of the maximum one. Secondly, as predicted by Eq. (2.3), the critical density should be $\rho_c = 59$ veh/km, thus the measured one appears to be very low.

The system is loading uniformly and has all features set uniformly. Let's try to make the same simulation decreasing the mean output flow of a street from 1 veh/km to 0.5 veh/km.

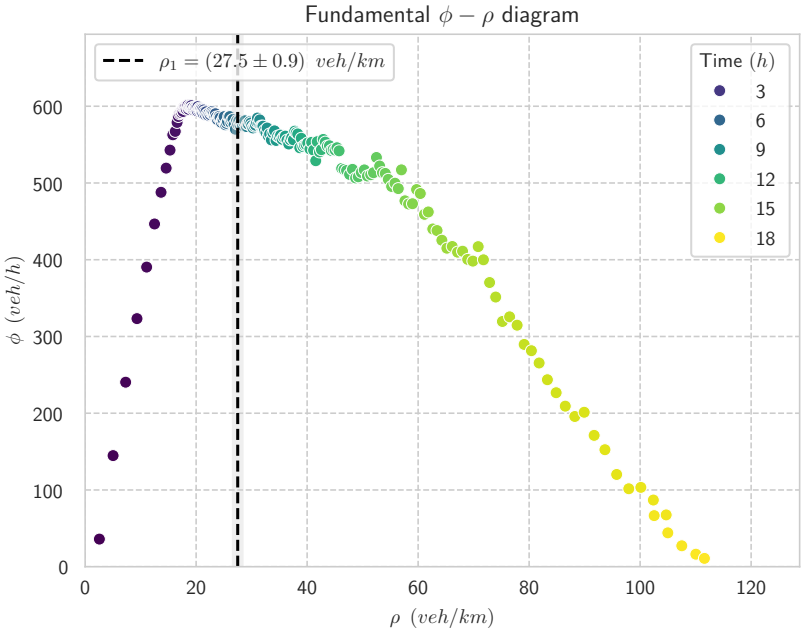

Figure 4.5: *Fundamental flow/density diagram for a stationary simulation on a network composed by traffic lights. Here the maximum street output flow has been reduced from* 1 veh/km *to* 0.5 veh/km. *The plot is the resulting average of five different simulations which have all the same parameters but the seed.*

From Fig. 4.5 one can see how reducing the output flow of streets increases the plateau length. The only explanation of such phenomenon has to be searched in the

network topology.

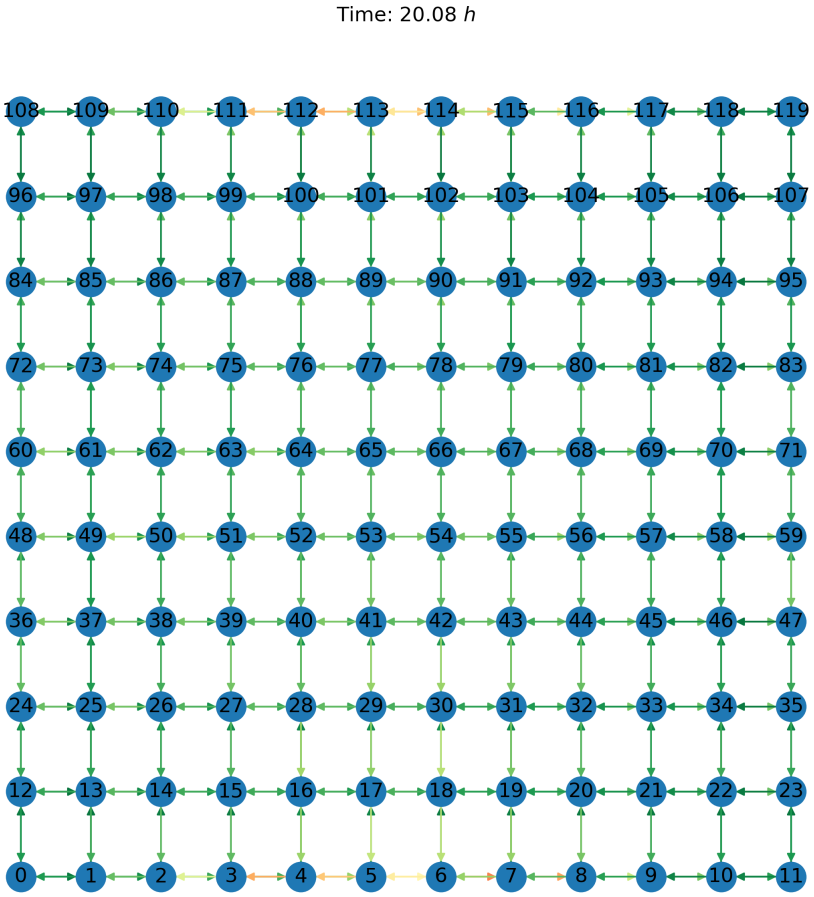

Figure 4.6: *Plot of the network road densities form the non-optimized simulation after* 20.08 *hours of simulations. The color map is green for densities close to* 0*, yellow to* 0.5 *and red to* 1*. The plot is the resulting average of five different simulations which have all the same parameters but the seed.*

As shown by Fig. 4.6, the streets which seems to load faster are the ones at the border. Thus, the Manhattan like network introduces a bias in the simulation, despite its regularity. However, this makes sense: the exits are all borders' nodes, so it is unlikely for a vehicle to be in the road network center.

Let's now try to repeat the previous analysis with the standard output flow and all parameters as the first one but the error probability, which is going to be increased from 5% to 30%.

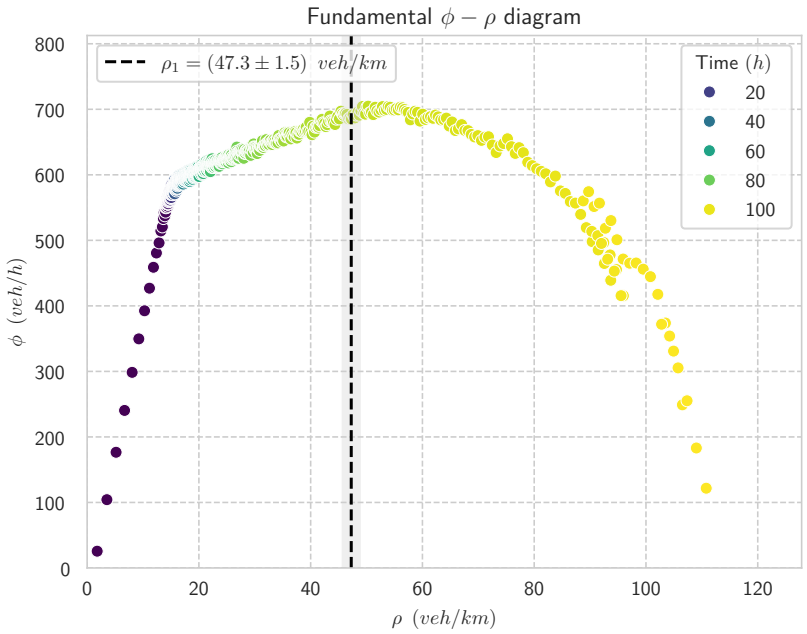

Figure 4.7: *Fundamental flow/density diagram for a stationary simulation on a network composed by traffic lights. Here the error probability has been set to* 30%. ρ_1 *corresponds to the density at which the formation of the Giant Component occurs, at time* (93.5 ± 1.3) h. *The plot is the resulting average of five different simulations which have all the same parameters but the seed.*

From Fig. 4.7 one is able to reduce topological effects just by increasing the error probability up to 30%. In fact, now the flow has it maximum at a density of about 60 veh/km, as predicted by the reference model.

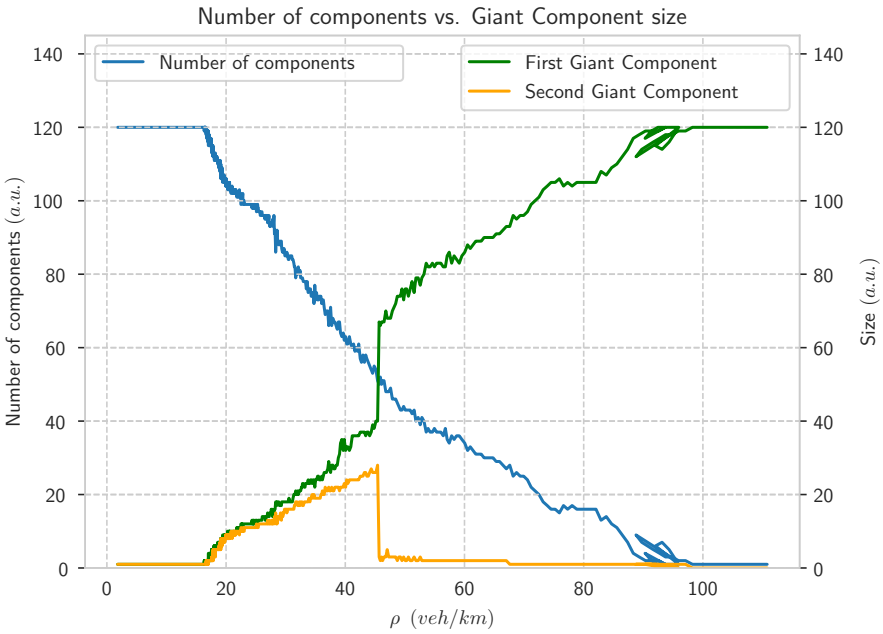

Figure 4.8: *Number of components with* $\theta_\rho = 1$ *versus the Giant Component size. Here the error probability has been set to* 30%. *The bigger delta is located at* $\rho = 47.3 \pm 1.5$ veh/km. *The plot is the resulting average of five different simulations which have all the same parameters but the seed.*

By looking at Fig. 4.8 one can see the Giant Component creation at $\rho = 40.8$ veh/km, corresponding to 93.5 ± 1.3 h. However, also in this case the flow fluctuations are giving 92.8 ± 1.5 h as congestion time, as shown in Fig. 4.9.

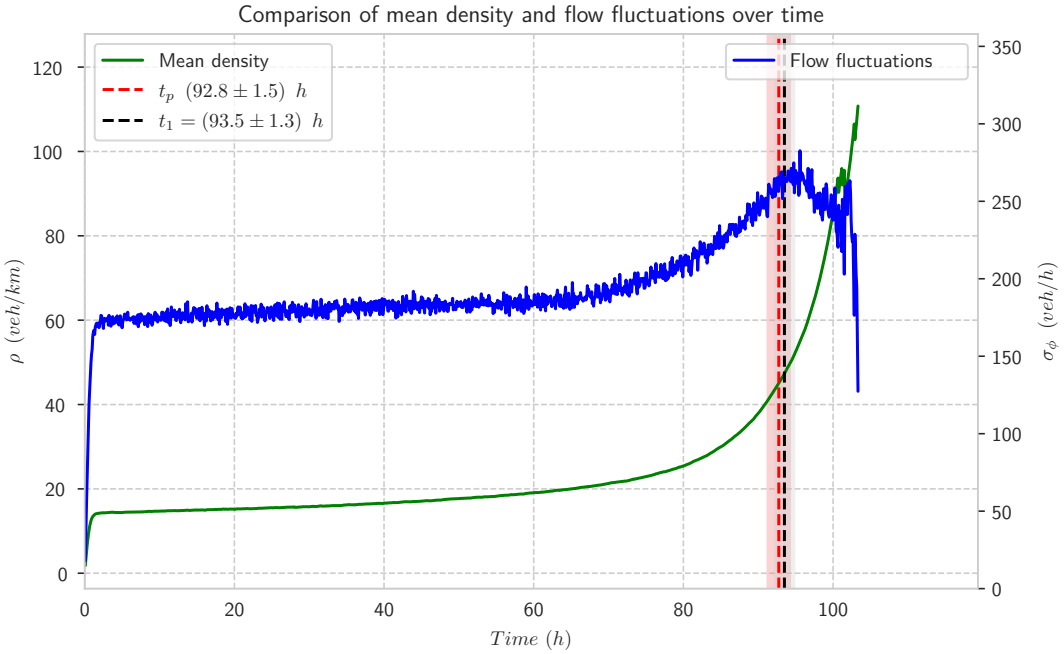

Figure 4.9: *Time plot of mean network density vs mean flow fluctuations. Here the error probability has been set to* 30%*. The parameters used for the peak detection algorithm are* $l = 500$*,* $t = 3$ *and* $i = 0$*.* t_1 *corresponds to the time at which the formation of the Giant Component occurs.* t_p *corresponds to the time at which the peak is detected. The plot is the resulting average of five different simulations which have all the same parameters but the seed.*

Let's try to look for another observable, e.g. assuming to have information only about vehicle density, instead of flow. In this case, the idea is that the normalized density fluctuations, i.e. the density fluctuations normalized by the mean, over the density will have a maximum when the formation of small clusters of congested streets occurs. This is expected to be slightly before the Giant Component creation, thus giving information about congestion formation. In Fig. 4.10 one can see that the maximum of density fluctuations, which occurs at time (85.3 ± 1.6) h against the Giant Component formation at time (93.5 ± 1.3) h. It was expected that density fluctuation maximum would appear before the signal given by flow fluctuations, due to the fact that at this maximum one has many small congested cluster and not yet a Giant Component.

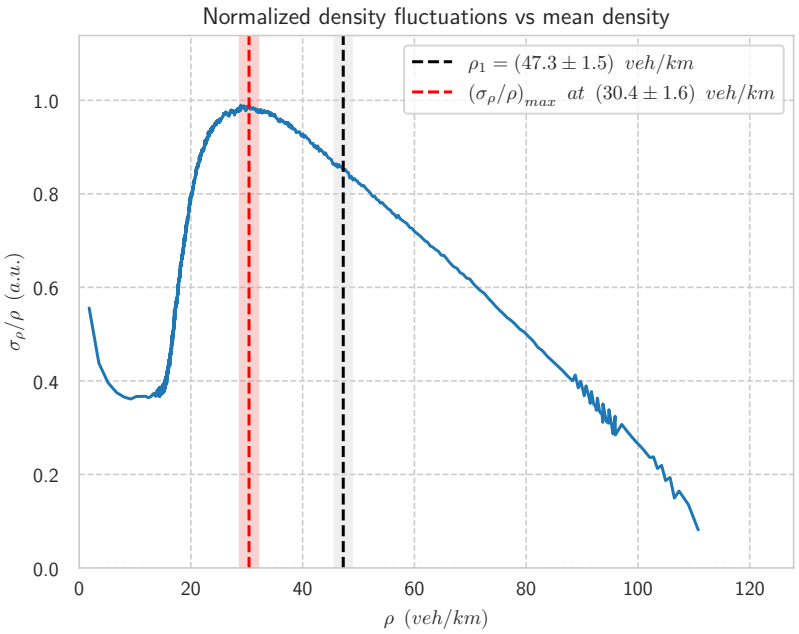

Figure 4.10: *Time plot of normalized density fluctuations vs mean density. Here the error probability has been set to* 30%. ρ_1 *corresponds to the density at which the formation of the Giant Component occurs.* $(\sigma_\rho/\rho)_{max}$ *occurs at time* (85.3 ± 1.6) h. *The black dashed line corresponds to the Giant Component formation.*

To validate this result, let's see what happened in the low error probability case, shown in Fig. 4.11. In this case, the maximum of $(\sigma_\rho/\rho)_{\max}$ occurs at time (39.6 ± 0.8) h. Recalling that in this case the Giant Component formation time was (40.8 ± 0.9) h, the estimation is perfectly coherent.

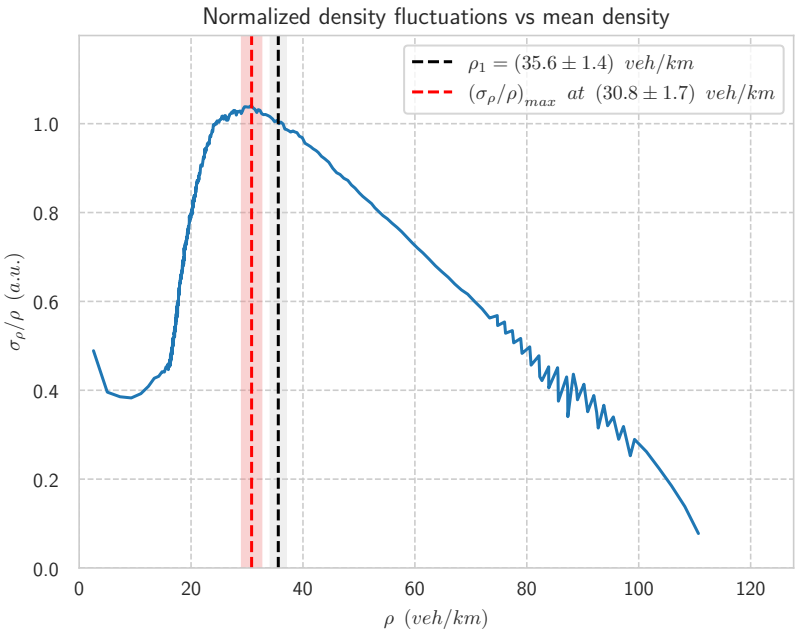

Figure 4.11: *Time plot of normalized density fluctuations vs mean density.* ρ_1 *corresponds to the density at which the formation of the Giant Component occurs.* $(\sigma_\rho/\rho)_{max}$ *occurs at time* (39.6 ± 0.8) h. *The black dashed line corresponds to the Giant Component formation.*

Finally, increasing the error probability seems to delay the formation of the Giant Component. This can be explained by noticing that increasing error probability is equivalent to increase the time of permanence in the network. Thus, vehicles stay in the center for a longer time, allowing the external streets to enter congestion later.

4.1.1 Optimization algorithm

At this point of the research, which is to understand how and when traffic jams occur in a Manhattan-like network with randomly regulated traffic lights, it is proposed to investigate the possibility of improving the resilience of the same network through traffic light regulation. This would involve leveraging the overall traffic flow at the corresponding density. In fact, the green and red times of a semaphore are being set arbitrarily, so one could think about time optimization. The easiest algorithm one could think relies on the queue length on the streets connected to the traffic light. At this point, there are two main schools of thought: increasing the green time for the congested streets, to let vehicles flow, or increasing the green time for non-congested streets, giving up on the congested ones. Notice that in both cases some vehicles are going to "pay the delay tax"

for others.

Having chosen a regular network, increasing red time for congested streets may not be the best solution: all roads are virtually equal so blocking the flow on two of them may trigger a chain reaction and collapse the entire network. Then, let's choose to optimize the congested streets. The implemented algorithm is going to take two parameters in input, the time interval of application Δt and a percentage threshold $r \in [0, 1]$. For each traffic light, let's sum up all vehicles of roads which are affected by the cycle in the same way, which will give two sums S_1 and S_2. At this point, if $|S_1 - S_2| > r \min\{S_1, S_2\}$, one can choose to change the traffic light cycle increasing the green time for the streets with more vehicles on them. The delta time is chosen by looking at the queues difference, i.e. the difference of vehicles effectively waiting at the junction

$$\Delta\tau = \frac{|Q_1 - Q_2|\, T}{\Delta t}$$

where T is the traffic light cycle duration. Both green and red times will change by $\Delta\tau$ depending on S_1 and S_2 length, meaning that the algorithm leaves the total cycle time T unchanged.

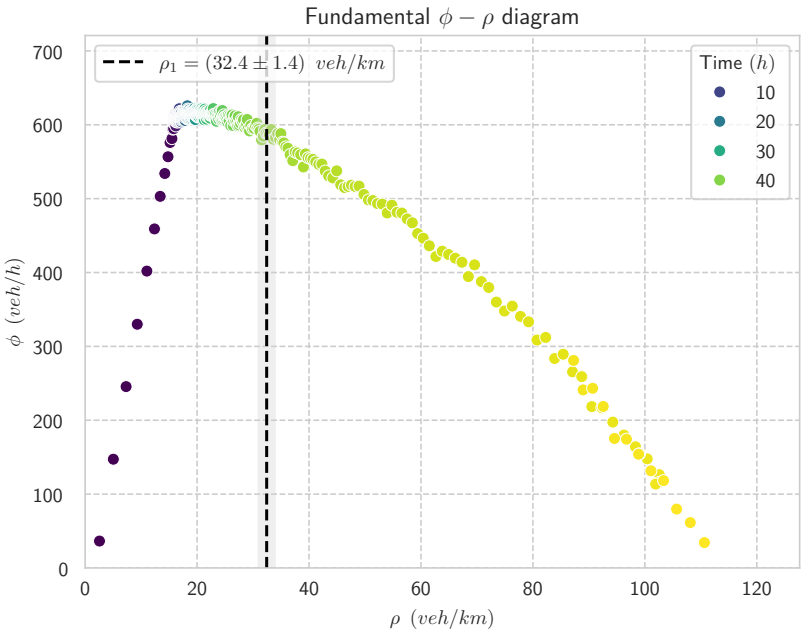

Figure 4.12: *Fundamental flow/density diagram for a stationary simulation on a network composed by traffic lights. Traffic lights are optimized every* 420 *s with a threshold of* 15%. ρ_1 *corresponds to the density at which the formation of the Giant Component occurs, at time* (41.3 ± 0.8) *h. The plot is the resulting average of five different simulations which have all the same parameters but the seed.*

In Fig. 4.12 is drawn the fundamental diagram for the optimized simulation. One can notice that the Giant Component in this case forms at a lower density with respect to the non-optimized case and, as expected, the curve is like the one represented in Fig. 4.1. This time the timescale is different, meaning that this simulation, with equal settings, was able to resist more time until the complete collapse. To better compare them, both are overlapped in Fig. 4.13. The previous plot at low error probability (5%) is represented by blue dots squares while the optimized one is represented by orange squares. In this case the algorithm seems not to be so effective, due to the complete overlap of the two curves.

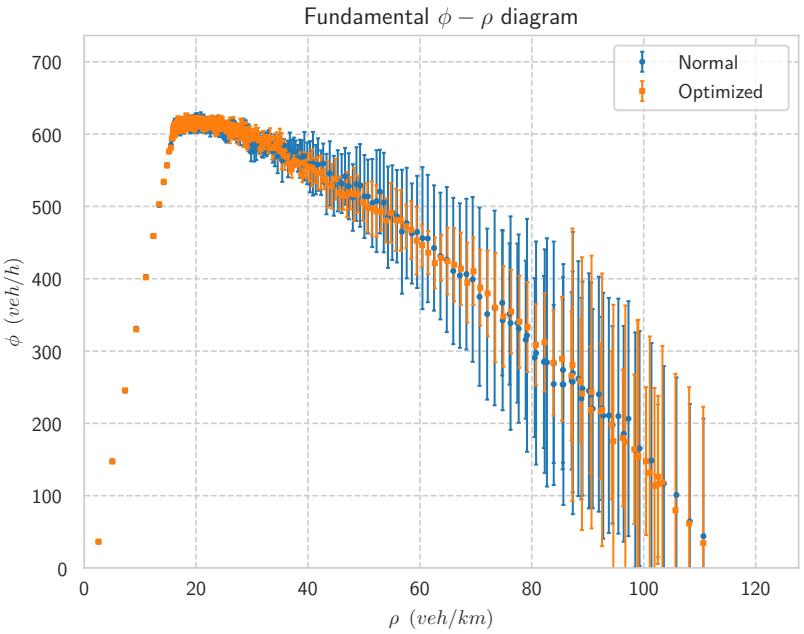

Figure 4.13: *Fundamental flow/density diagram for a stationary simulation on a network composed by traffic lights. Traffic lights are optimized every* 420 *s with a threshold of* 15%. *The error bars are the standard deviation of the five simulations done for both normal and optimized cases.*

To see if something is really changing let's have a look at the density fluctuations in Fig. 4.14. From a theoretical point of view, fluctuations should decrease but also in this case the two curves overlap each other. Notice that the error bars are not the fluctuations but the standard deviation of the mean computed for five simulations. At higher density, error becomes larger because the end time of simulation varies basing on random conditions, thus for longer times one has more divergence.

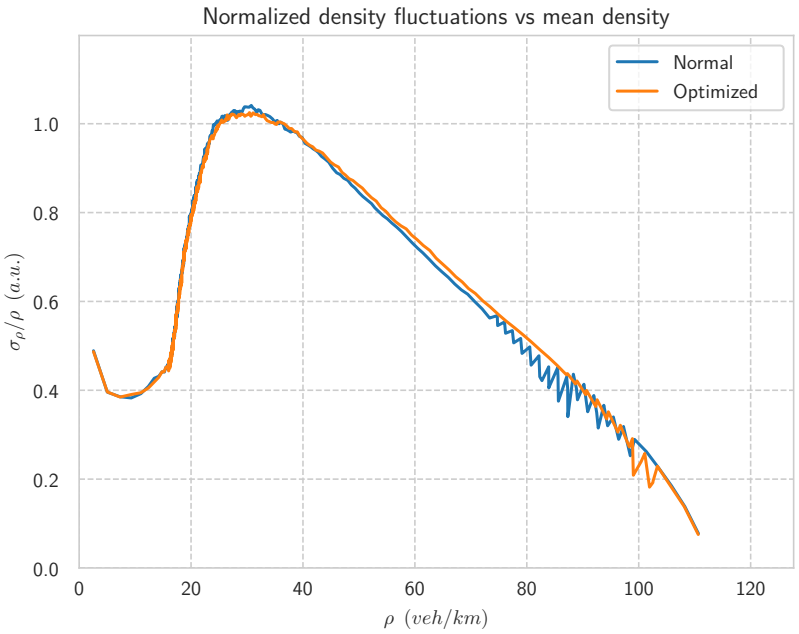

Figure 4.14: *Time plot of normalized density fluctuations vs mean density. Traffic lights are optimized every* 420 *s with a threshold of* 15%*. The plot is the resulting average of five different simulations which have all the same parameters but the seed.*

In Fig. 4.15 is shown the plot of the flow fluctuations and in Fig. 4.16 the plot of density fluctuations. In both cases, the forecasting property of fluctuations has not changed.

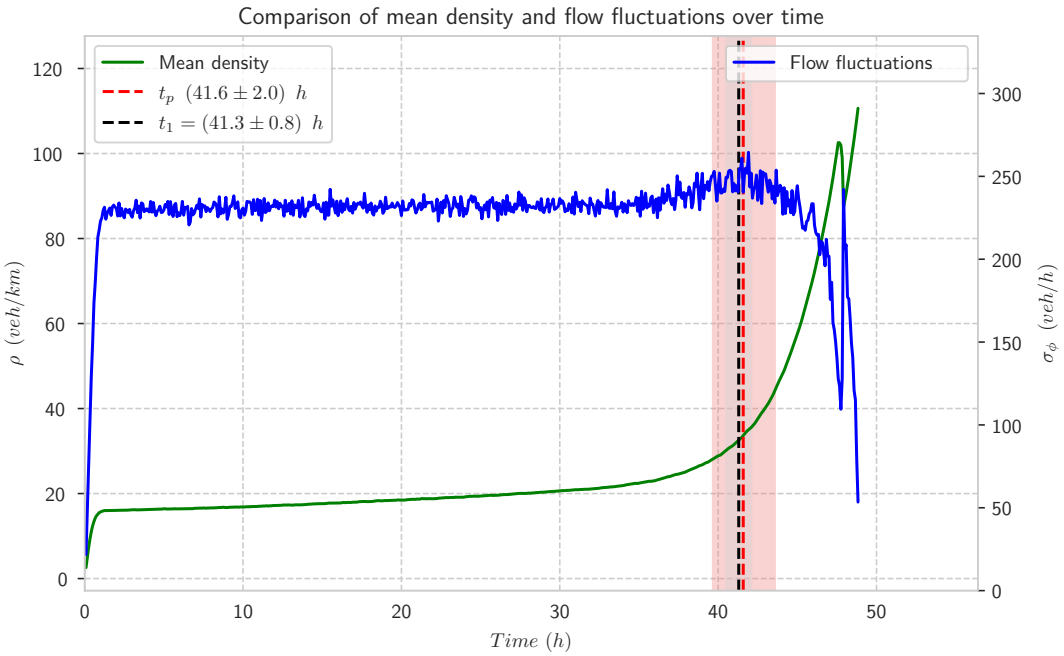

Figure 4.15: *Time plot of mean network density vs mean flow fluctuations for an optimized traffic light network. Traffic lights are optimized every* 420 *s with a threshold of* 15%. *The parameters used for the peak detection algorithm are* $l = 500$, $t = 5$ *and* $i = 0$. t_1 *corresponds to the time at which the formation of the Giant Component occurs.* t_p *corresponds to the time at which the peak is detected. The plot is the resulting average of five different simulations which have all the same parameters but the seed.*

By now, only the simulation with low error probability has been optimized, without any success... What may happen by optimizing one simulation with higher error probability?

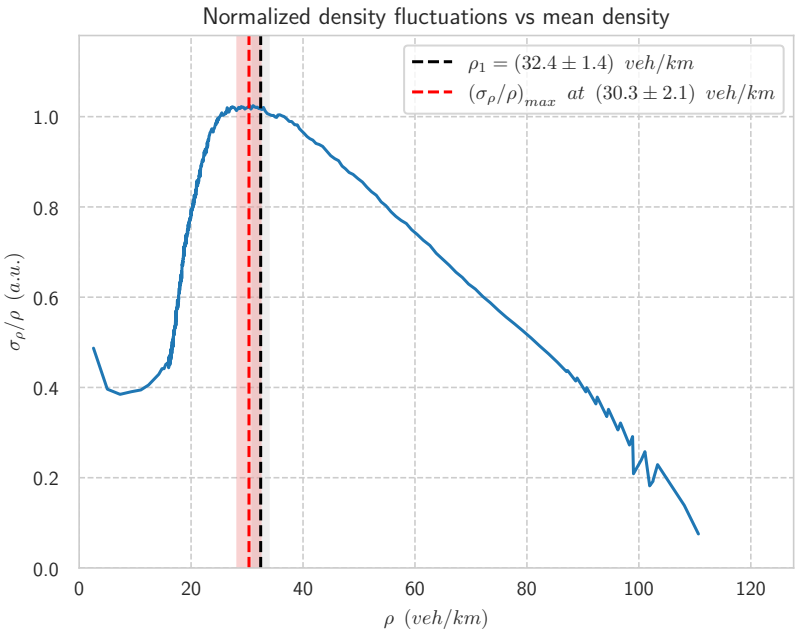

Figure 4.16: *Time plot of normalized density fluctuations vs mean density. Traffic lights are optimized every* 420 *s with a threshold of* 15%. ρ_1 *corresponds to the density at which the formation of the Giant Component occurs.* $(\sigma_\rho/\rho)_{max}$ *occurs at time* (40.6 ± 1.5) *h. The plot is the resulting average of five different simulations which have all the same parameters but the seed.*

In order to answer the previous question, let's reconsider a simulation in which agents have 30% error probability comparing it with the optimized one. As one can see in Fig. 4.17 and Fig. 4.18, fluctuations are slightly reduced in this case, but also the flow is lower if compared with the system's load. The reduction of fluctuations for the same load indicates that the algorithm is working. However, being the flow at equal load averagely lower, an algorithm of this type does not handle well congested states.

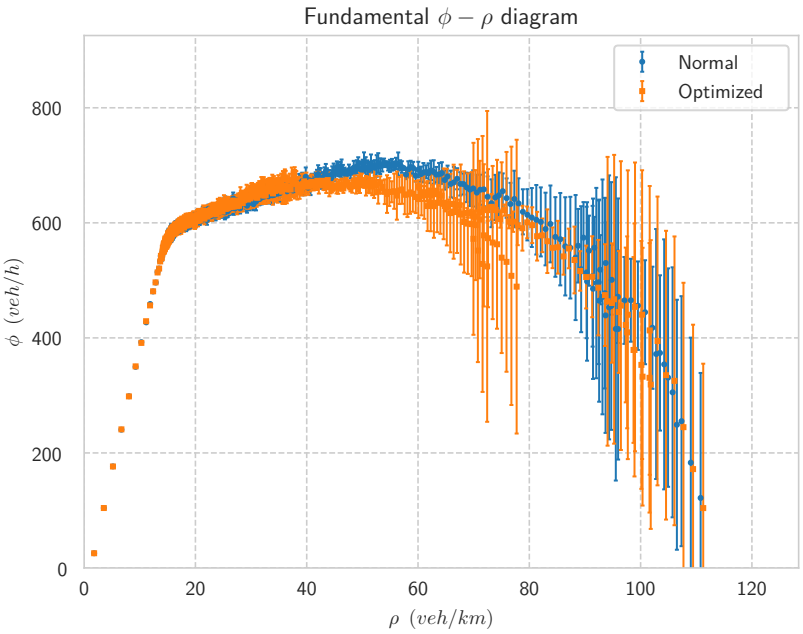

Figure 4.17: *Fundamental flow/density diagram for a stationary simulation on a network composed by traffic lights. Here the error probability has been set to* 30%. *Traffic lights are optimized every* 420 *s with a threshold of* 15%. *The error bars are the standard deviation of the five simulations done for both normal and optimized cases.*

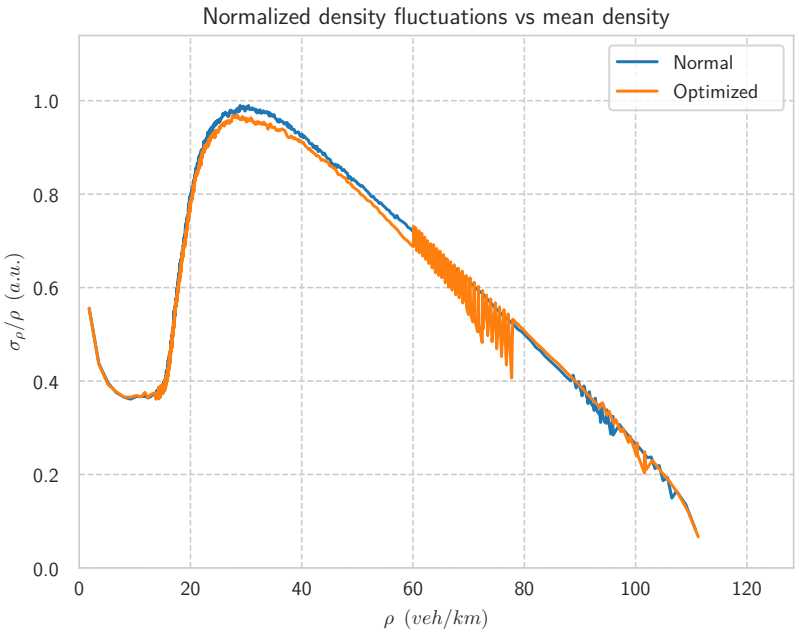

Figure 4.18: *Time plot of normalized density fluctuations vs mean density. Here the error probability has been set to* 30%. *Traffic lights are optimized every* 420 *s with a threshold of* 15%. *The plot is the resulting average of five different simulations which have all the same parameters but the seed.*

4.2 Roundabouts

As final study, let's take the road network in Fig. 4 setting every junction as a roundabout. Recall that, as seen in Sec. 3.2.2, roundabouts have a FIFO structure, so they do not have a priority rule. Traffic lights allow, on average, a flow of 2 vehicles per time step. However, as discussed in implementation (Sec. 3.2), a roundabout handles a flow up to 4 vehicles per time step, which is double. In order to make traffic lights and roundabouts results comparable, the streets' output flow has been reduced as in the previous section. Furthermore, due to the FIFO nature of roundabouts, to have an average flow of 2 vehicles per time step for a single node one must find the probability to move (p) which solves the equation

$$\sum_{i=1}^{d} p^i = 2$$

where d is the degree of the node. Making a weighted average based on the degree of the nodes, one can find that the probability at which the desired flow is obtained corresponds

to $p = 77.07\%$. Firstly, let's look at the fundamental diagram of the simulation shown in Fig. 4.19.

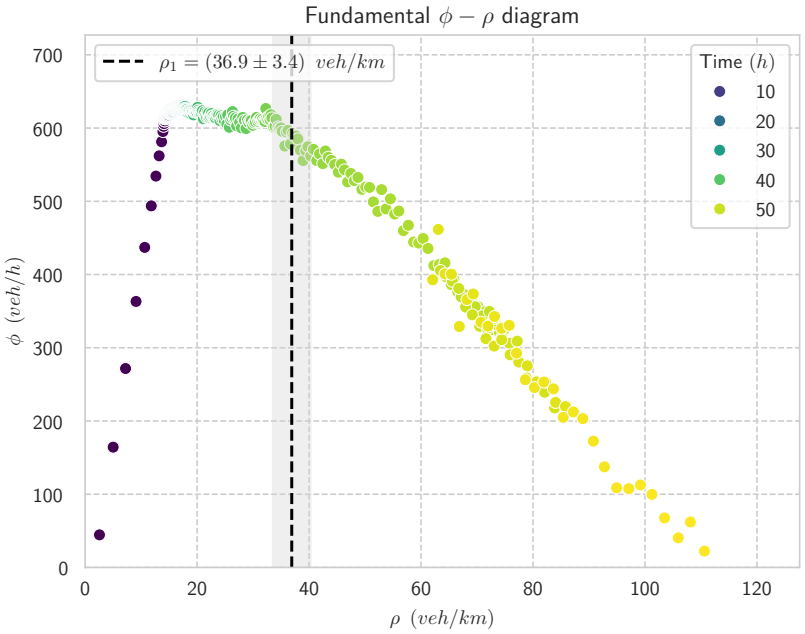

Figure 4.19: *Fundamental flow/density diagram for a stationary simulation on a network composed by roundabouts. The maximum street output flow has been reduced from* 1 *veh/km to* 0.7707 *veh/km.* ρ_1 *corresponds to the density at which the formation of the Giant Component occurs, at time* (45.0 ± 2.2) *h. The plot is the resulting average of five different simulations which have all the same parameters but the seed.*

As in the traffic lights analysis, one can see that at low densities, the flow/density relationship is linear as predicted by Eq. (1.2). Then, as hypothesized in Eq. (2.2), a plateau is reached and one has a nearly constant flow for many density values. As before, after the plateau the congestion occurs causing the flow to decrease while the density increases. Notice that after a density of 80 *veh/km* a quick drop appears: this is due to the fact that roundabouts tend to congest at high density, unlike traffic lights.

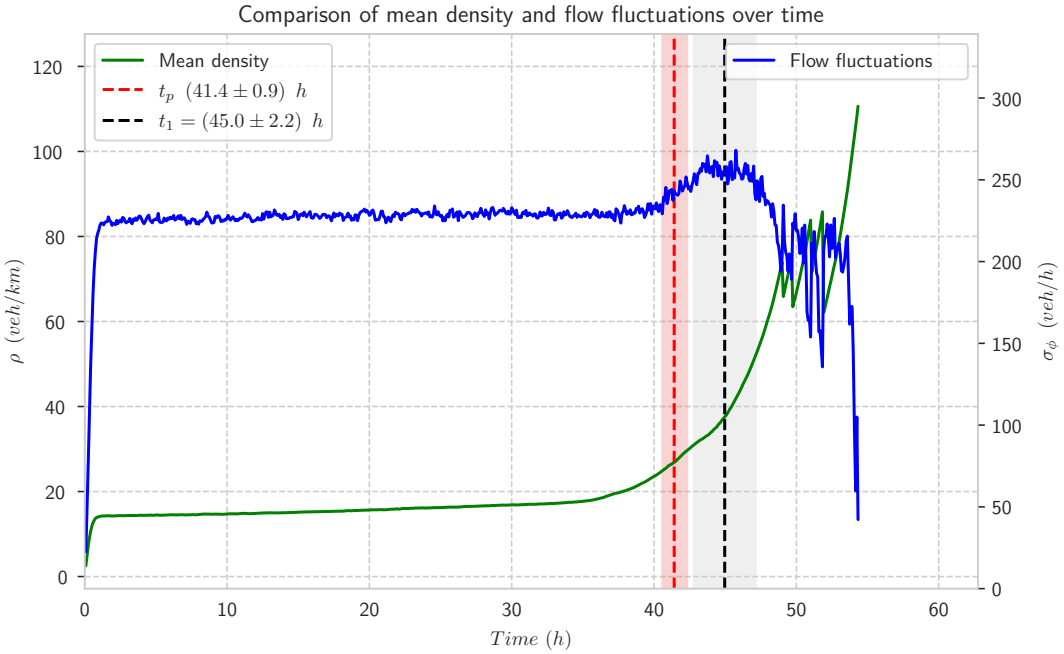

Figure 4.20: *Time plot of mean network density vs mean flow fluctuations. The maximum street output flow has been reduced from* 1 *veh/km to* 0.7707 *veh/km. The parameters used for the peak detection algorithm are* $l = 500$, $t = 5$ *and* $i = 0$. t_1 *corresponds to the time at which the formation of the Giant Component occurs.* t_p *corresponds to the time at which the peak is detected. The plot is the resulting average of five different simulations which have all the same parameters but the seed.*

In Fig. 4.20 one can compare the plot of the mean density and the mean flow fluctuations over time. The flow fluctuations have a lower average value and are more stable with respect to traffic lights, which is an advantage of using roundabouts. In this case, the peak detected by the algorithm is almost compatible with the Giant Component formation, with a time of (41.4 ± 0.9) h against (45.0 ± 2.2) h. Moreover, the density fluctuation maximum shown in Fig. 4.21 reports a compatible time of (41.1 ± 1.6) h. In this case, the maximum is higher with respect to traffic lights because roundabout junctions tends to congest as well as the streets at high densities. In fact, at the same time one has a different density: this could be due to the gridlock formation which can happen in the roundabout case. Indeed, traffic lights always permit the passage of some vehicles while roundabouts are forced to move the first vehicle first. Thus, if such vehicle cannot move the whole node is locked, and this effect propagates quickly through the whole net. Finally, this effect is visible also at high densities in Fig. 4.20, where the mean is highly fluctuating due to low data availability (only five simulations were done)

and high gridlock dependence.

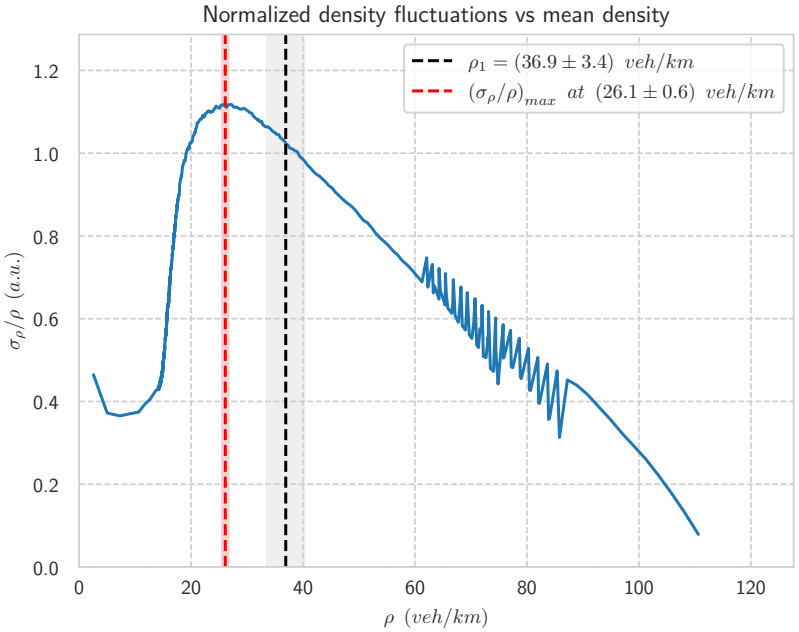

Figure 4.21: *Time plot of mean network density vs mean flow fluctuations. The maximum street output flow has been reduced from* 1 veh/km *to* 0.7707 veh/km. ρ_1 *corresponds to the density at which the formation of the Giant Component occurs.* $(\sigma_\rho/\rho)_{max}$ *occurs at time* (41.1 ± 1.6) h. *The plot is the resulting average of five different simulations which have all the same parameters but the seed.*

One can conclude that, given a system in a stationary state, flow fluctuations could be a predictor of a phase transition, i.e. a passage from a free to a congested state. In particular, both flow and density fluctuations seem to give reliable results, thus for a real application it would be ideal to have both data sources to analyze.

Chapter 5

Simulation results in non-stationary conditions

The aim of this chapter is to study how the traffic model developed in this work behaves in non-stationary conditions. An application on a real road, namely *Via Stalingrado* in Bologna, is discussed in Sec. 5.1. The result is a coherent response to an external dynamical input by both traffic lights and roundabout. Then, results from a Manhattan-like network composed by traffic lights (Sec. 5.2) or roundabouts (Sec. 5.3) are discussed, both showing a reasonable response to a dynamical input.

5.1 The "strange" case of *Via Stalingrado*

One of the earliest studies done using the model from this work was done on *Via Stalingrado*, which is a street in Bologna with some characteristics which makes it good to simulate:

- It is a straight connection between the suburbs and the city center, connecting the freeway of Bologna to the *Viali*;
- It has many traffic lights, thus it could be good for quantifying their effects on traffic;
- It has many loops on it, even though many of them are not working properly therefore it became necessary to make some workaround.

In Fig. 5.1 a cartography of Bologna is shown, highlighting *Via Stalingrado* with a black line. Real data come from the loops highlighted with blue markers. In particular, the marker over *Via Stalingrado* is a loop from *Comune di Bologna* measuring vehicle passages from the suburb to the *Viali*. The further loop is instead from *Regione Emilia-Romagna* and counts vehicle passages in the same direction. From now on, let's denote

with C the *Comune*'s loop and R the *Regione*'s loop. The necessity of doing a simulation came from a strange behavior revealed by C data which seemed to show a cut with respect to the input trend measured by R. Notice that, despite the high number of loops on *Via Stalingrado*, C and R were the closest one correctly working. Moreover, in order to do a simulation one needs data aggregated within a decent time window, which could be one up to five minutes.

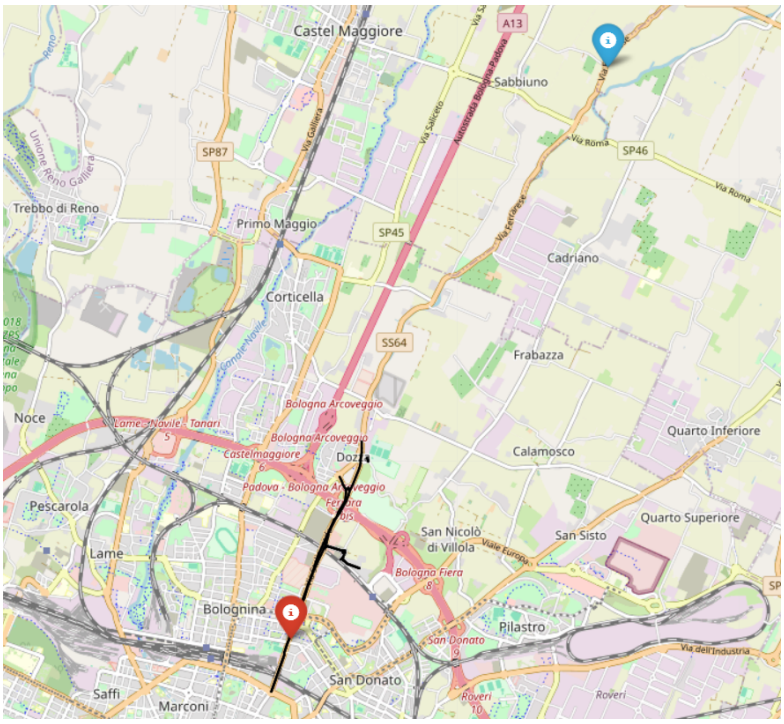

Figure 5.1: *Cartography of Bologna. The black line is Via Stalingrado. The blue marker is R, the loop from Regione Emilia-Romagna, located in Via Ferrarese. The red marker in Via Stalingrado is C, the loop from Comune di Bologna.*

Unfortunately, all data coming from C were aggregated to one hour, making them useless, with except to the one measured on 8 January 2024 which are aggregated at five minutes. However, the loop R was not working correctly on that specific day, so the input data, aggregated at one minute, were measured on 24 May 2023. Due to limitations imposed by data the following simulation and analysis are not going to be a good representation of reality. One can still take it qualitatively, using it to show the traffic light effect on the flow load shape.

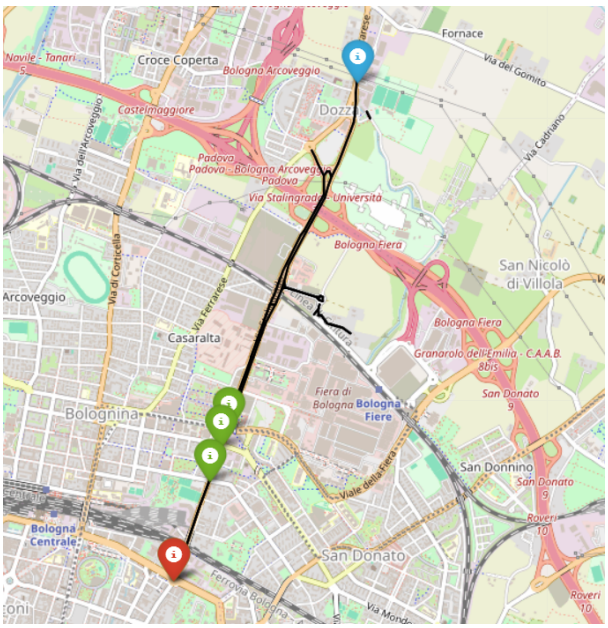

Figure 5.2: *Cartography of a custom models of Via Stalingrado (black line). Green markers are traffic lights. The blue marker is the virtual position of R. The red marker is the virtual position of C. Notice that a traffic light coincides with C and that the road considered in the simulations consists only of the straight line connecting R and C.*

Let's now build a model for the simulation, schematized in Fig. 5.2, taking into account many approximations:

- The input flow will be the one measured by R, thus assuming that the flow shape is defined and accounting that it could change amplitude while going to *Via Stalingrado*;
- The output flow used for comparison will be the one measured by C;
- The simulation will ignore contributions coming from lateral roads, assuming a sort of detailed balance;
- The model consists of four traffic lights and four street segments.

In particular, street segments ordered starting from the closest one to *Via Ferrarese* have lengths of 2281, 118, 222 and 651, expressed in meters. In the same order, traffic lights have the following green-red time pairs: (62, 70), (72, 69), (88, 50) and (81, 50), expressed in seconds.

5.1.1 Predicted vs Observed flow

Firstly, let's have a look to the difference between the flow measured by C (ϕ^{obs}) and the flow predicted by the model (ϕ^{th}) given the input of R.

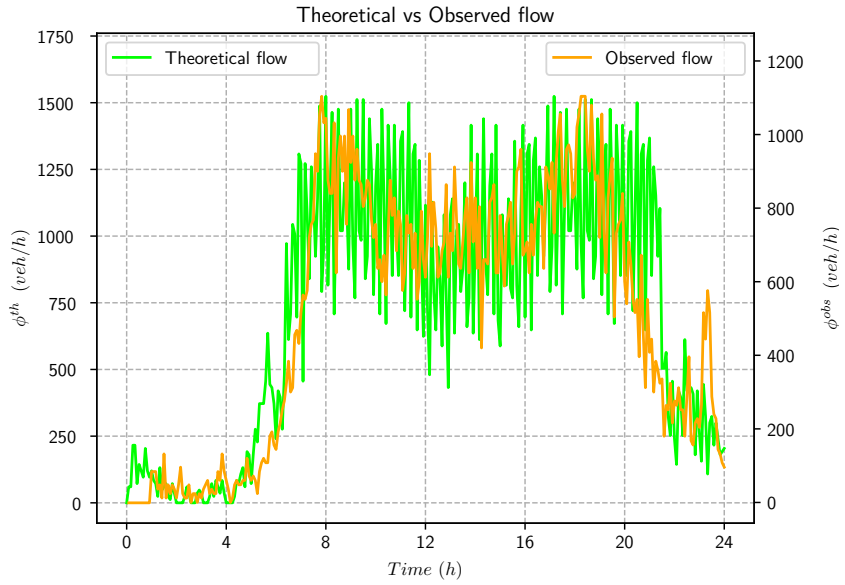

Figure 5.3: *Comparison between the observed flow and the flow predicted by the model. The input flow consists of data acquired on 24 May 2023 by R. The output reference (orange) consists of data acquired on 8 January 2024 by C. In green, the output predicted by the model.*

From Fig. 5.3 one can see immediately the similarity between theoretical (predicted) and observed flows. As expected, ϕ^{th} has a greater amplitude with respect to ϕ^{obs} due to the assumption did at the beginning of this section. Moreover, the observed flow appears slightly delayed with respect to the input one, due to the transit time required by the road itself. To understand what is particular in this plot, let's look at Fig. 5.4.

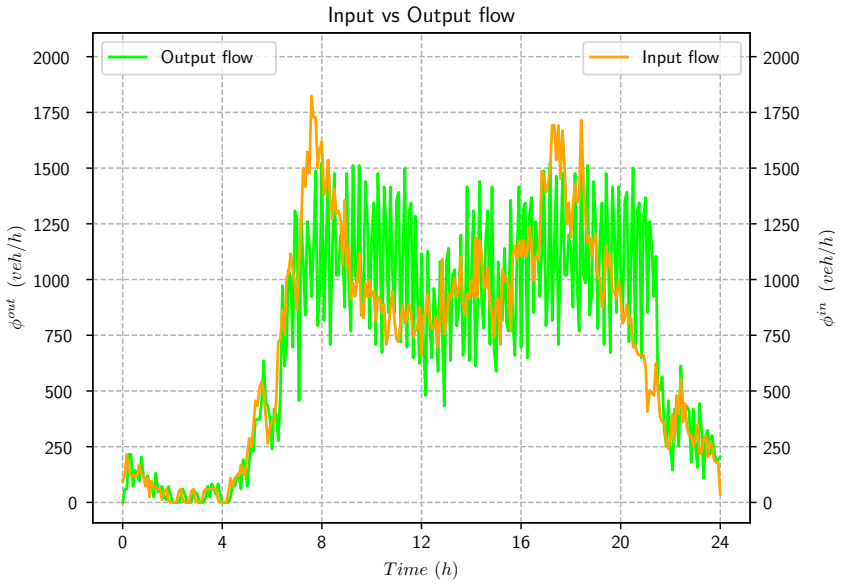

Figure 5.4: *Comparison between the input flow (orange), acquired on 24 May 2023 by R, and the output flow (green), predicted by the model.*

Here one can see how the input flow shape is cut by some effect due to *Via Stalingrado*. As saw previously in From Fig. 5.3, traffic lights could be the cause of this phenomenon.

5.1.2 Traffic Lights vs Roundabouts

To validate the previous results, the next simulation will be an exact copy of the previous one but for the junctions, which are all set to be roundabouts. As one can see from Fig. 5.5, the output coming from roundabouts has the same shape of the input despite being measured at the same point in the simulation with respect to the one with traffic lights. Notice also that its peak is much higher as the traffic lights' one, meaning that a network consisting of roundabouts is capable to manage loads smoothly. This is due to the fact that, by ignoring lateral vehicle influences, roundabouts make the system act like a unique street. On the other hand, traffic lights obey a green-red cycle, thus blocking the road independently on the presence or absence of lateral incoming vehicles. This justifies the flatter and more fluctuating trend of the traffic lights curve with respect to the roundabouts one.

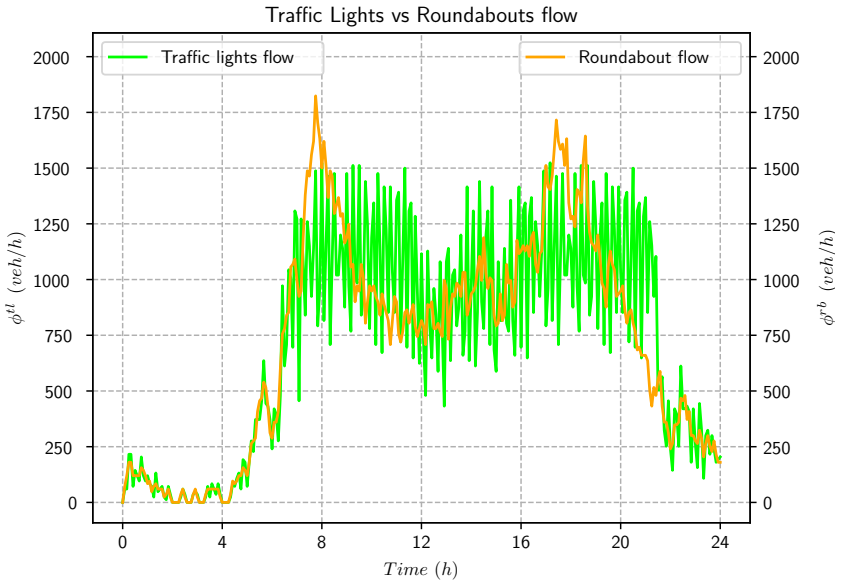

Figure 5.5: *Comparison between the flow produced by traffic lights (green) and the one produced by roundabouts (orange). The input flow consists of data acquired on 24 May 2023 by R.*

Finally, one can conclude that the model well represents the reality, thus not having sufficient data to do a more accurate study. From the analysis, it becomes clear that the observed cut at the end of *Via Stalingrado* is an effect of the traffic lights dynamics. By replacing traffic lights with roundabouts, one can restore the original shape of the input. Notice that the only aim of this paragraph is to show the effects of traffic lights on a simple road network. It is not proposing a solution to a problem as many strong assumptions were made at the beginning, thus it just works as toy model.

5.2 Traffic Lights

In the Sec. 5.1 the model has been tested on a real street using real data. However, despite the results were realistic, it is still a single street. To test the model further, let's recall the Manhattan-like network previously shown in Fig. 4 and test it using the input flow shape measured by the R loop. In particular, let's take the same traffic light network used in Sec. 4.1, setting the input to the flow measured by R multiplied by a factor of 31 to adapt to the network size. Due to the non-stationary nature of the simulation, some previous analyses are not going to give nice results, like the peak detection as congestion forecaster. Firstly, let's have a look to the mean network density vs the input flow

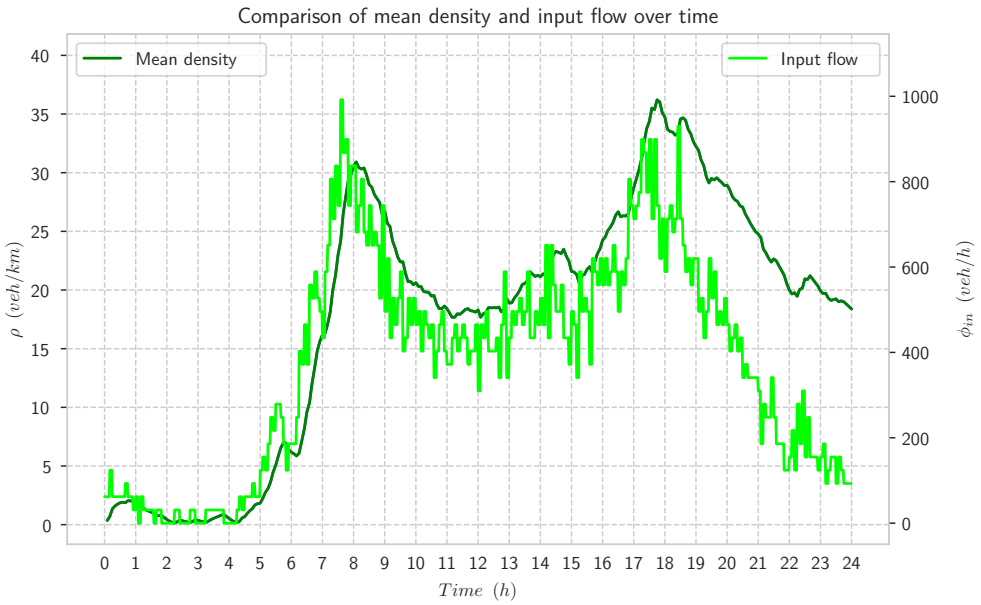

Figure 5.6: *Comparison between mean network density and input flow over time. The input flow consists of data acquired on 24 May 2023 by R multiplied by a factor of* 31.

From Fig. 5.6 the choice of the amplification factor (31) is justified: there is a delay from loading and unloading phases. Thus, the mean density remains high for some time after the evening peak, highlighting a congestion. Notice that both morning and evening peak overloads the system, but in the first case the system starts from an empty condition and the loading time is not sufficient to create a congestion. In the second case, instead, the systems starts already loaded from the morning, which allows the second input peak to create a congestion. Moreover, in Fig. 5.7 the fundamental flow/density diagram is shown. One can notice that the diagram presents two hysteresis cycles, one corresponding to the morning peak (around 8) and one corresponding to the evening peak (around 17). Notice also that the cycle does not complete, i.e. it does not return to the initial state, due to the high load which stressed the system.

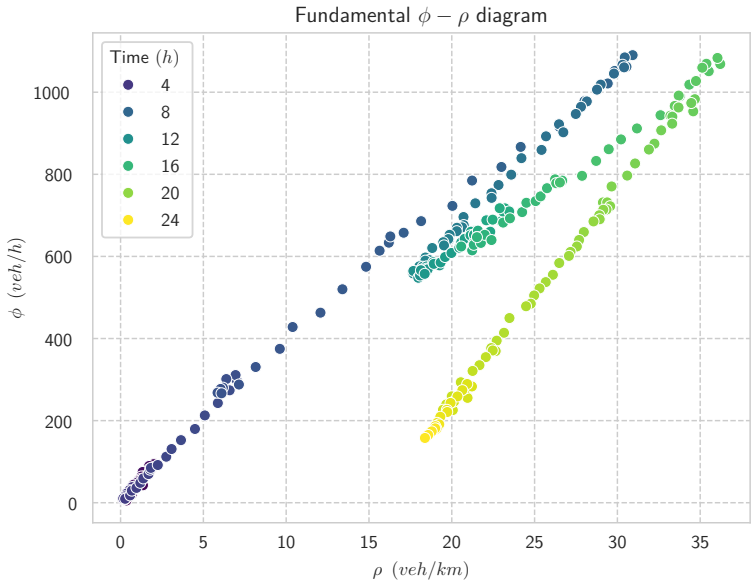

Figure 5.7: *Fundamental diagram with a dynamic network loading.*

5.3 Roundabouts

As discussed before, let's briefly see the previous result in the case of a network consisting of only roundabout nodes. As one can see from both mean density plot (Fig. 5.8) and the fundamental flow/density diagram (Fig. 5.9), the behavior of the system is remarkably like the traffic lights' one. Notice that also in this case the first peak is already overloading but not sufficient to cause a congestion starting from an empty system. Furthermore, the mean density in a non-congested state is slightly lower in the roundabout case: this fact highlights how, a part of input flow, roundabouts seem more efficient in allowing vehicles to exit the system when it is in a free state.

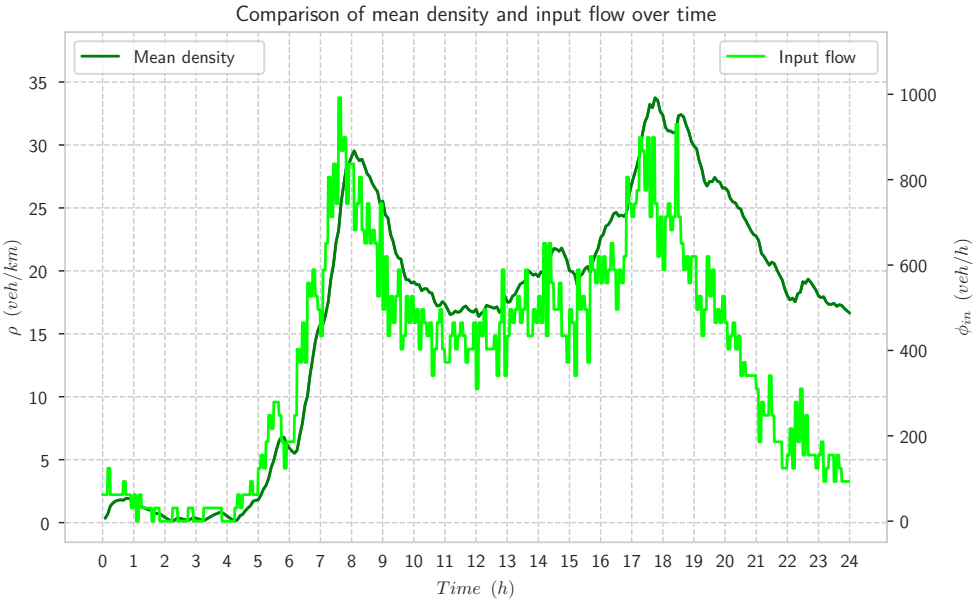

Figure 5.8: *Comparison between mean network density and input flow over time. The input flow consists of data acquired on 24 May 2023 by R multiplied by a factor of* 31.

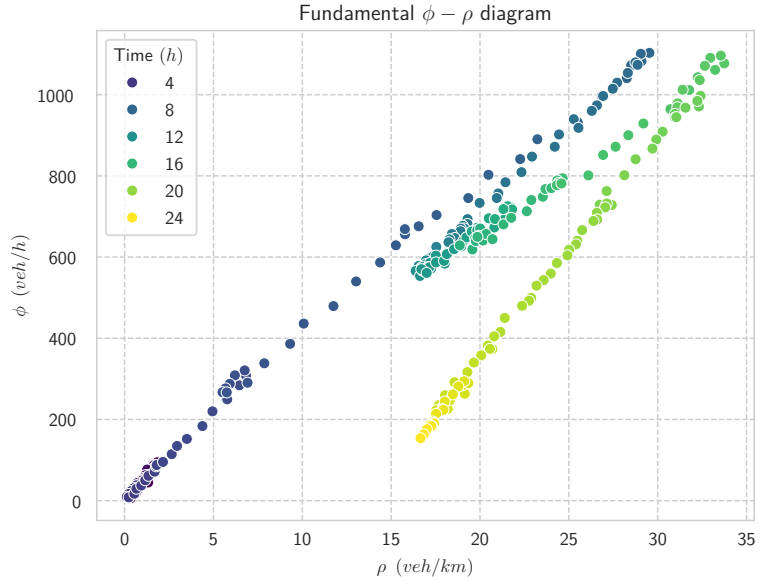

Figure 5.9: *Fundamental diagram with a dynamic network loading.*

Chapter 6

Discussion

In this work, a mesoscopic traffic model has been developed in order to understand congestion formation and to highlight predictive observables for such phenomenon. Traffic congestion can be explained as a percolation in a dynamical system on a network structure because of existence of finite transport rate at crossing points and finite road capacity. In this case, congestion on a road network is related to the formation of a Giant Component of streets with $\theta_\rho = 1$ as defined by Eq. (4.1). Once developed the model from both a theoretical perspective and an implementation standpoint, many analyses have been carried out on a Manhattan-like road network (Fig. 4). A set of analyses aimed at studying some observables as traffic congestion forecasters has been performed on a system in a quasi-stationary state, meaning that the networks has slowly and constantly been loaded with vehicles trying to keep the mean density almost constant. From such analyses, both flow fluctuations and normalized density fluctuations showed a good forecasting behavior in both traffic lights only and roundabouts only simulations. Moreover, the prediction was not influenced by parameters like the existence of a random dynamics for the vehicles. For what concerns traffic lights, an optimization algorithm has been implemented to enhance the network performances by changing green and red timings keeping all cycles durations constant. Such algorithm is based on the vehicle density on streets and showed remarkable results in reducing density fluctuations, as one would have expected. However, it showed poor performances with regard to vehicle flow over load. In fact, while the algorithm was working the mean density of the network tended to rise, resulting in a lower flow. Next, an analysis on *Via Stalingrado* has been performed, using real input data to generate synthetic data to compare with magnetic loops count. Despite not having availability of data for the same day, the model well reproduced the behavior of the traffic lights series on that street. Finally, the same input data were given to the Manhattan-like network, multiplied by a scaling factor, in order to study the behavior of such net with the system in a non-stationary state. The results were good in both traffic lights and roundabouts cases, with the roundabout being able to keep the average density lower with respect to traffic lights.

Starting from this work, many study paths can be followed. One of them could be finding a better optimization algorithm for traffic lights, which is able to decrease fluctuations while increasing flow for a given load, thus increasing transport capacity near congested states. The previous analyses were performed assuming to have a magnetic loop on each street, which is very unlikely (and costly) to have in a real setup. Thus, one could study what is the minimum number of loops to be placed randomly to gain the same forecasting properties of observable with respect to the full availability. Moreover, the Manhattan-like network has been chosen for its generality to reduce potential geometrical biases. Consequently, one may apply the model to any type of network in order to study it, being also able to implement it into the Digital Twin of a city. Finally, the fluctuations showed great forecasting capacity if the system is in a stationary state while giving no information at all for a system in a non-stationary state. A method is also required to make prediction for such systems, because they made up almost all real situations. One possible step forward could be creating a forecasting analysis based on more than one observable, taking advantage of artificial intelligence to manage multiple input peak detection.

Appendix A

Peak detection algorithm

The algorithm used for the peak detection is a robust peak detection algorithm based on z-score [29]. In particular, the algorithm gives a signal (which corresponds to a one) whenever a new data point is given at x standard deviations from the signal mean. It is based on three parameters:

- *Lag*: the length of the moving window computing mean and standard deviation of historical data. E.g. a lag of l means that the historical mean and standard deviation are computed considering the last l data points;
- *Threshold*: the z-score used by the algorithm. Calling x a new data point and μ, σ the moving mean and standard deviation of data, a signal is emitted when $|x - \mu| > z\sigma$, where z is the chosen threshold. So, z represents the number of standard deviations a point is away from the mean.
- *Influence*: the influence i is a constrained parameter ($i \in [0, 1]$). It represents the influence of the signal with respect to a new data point. Thus, an influence $i = 0$ assumes stationarity, giving the new data point the same influence of all other data.

Here it is the pseudocode

```
# Let y⃗ : |y⃗| ≥ l + 2 timeseries
# Let 𝔼 the mean operator
# Let std() be the standard deviation function
# Let |x| be the absolute value function for x

# Settings
set l to ...; # lag
set t to ...; # threshold
set i to ...; # influence
```

```
# Initialize variables
set $\vec{s} = \vec{0} : |\vec{s}| = |\vec{y}|$ # Initialize signal results
set $\vec{f}_y = (\vec{y}_1, \ldots, \vec{y}_l)$ # Initialize filtered series
set $\vec{\bar{f}}$ to null; # Initialize average filter
set $\vec{\sigma_f}$ to null; # Initialize std. filter
set $\vec{\bar{f}}_l = \mathbb{E}[\vec{y}]$; # Initialize first value average
set $\vec{\sigma}_{f_l} = std(\vec{y})$; # Initialize first value std.

for $j = l+1, \ldots, k$ do
if $\left|\vec{y}_j - \vec{\bar{f}}_{j-1}\right| > t\vec{\sigma}_{f_{j-1}}$ then
    set \vec{s}_{j} = 1;    # Positive signal
    end
    set $\vec{f}_{y_j} = i\vec{y}_j + (1-i)\,\vec{f}_{y_{j-1}}$;
else
    set $\vec{f}_{y_j} = \vec{y}_j$;
end
set $\vec{\bar{f}}_j = \mathbb{E}\left[\vec{f}_{y_{j-l+1}}, \ldots, \vec{f}_{y_j}\right]$;
set $\vec{\sigma}_{f_j} = std(\vec{f}_{y_{j-l+1}}, \ldots, \vec{f}_{y_j})$;
end
```

Bibliography

[1] J. Kwapień and S. Drożdż, "Physical approach to complex systems," *Physics Reports*, vol. 515, no. 3, pp. 115–226, 2012, Physical approach to complex systems, ISSN: 0370-1573. DOI: https://doi.org/10.1016/j.physrep.2012.01.007. [Online]. Available: https://www.sciencedirect.com/science/article/pii/S0370157312000166.

[2] F. L. Ribeiro, M. Perc, and H. V. Ribeiro, "Editorial: The physics of cities," *Frontiers in Physics*, vol. 10, 2022, ISSN: 2296-424X. DOI: 10.3389/fphy.2022.964701. [Online]. Available: https://www.frontiersin.org/articles/10.3389/fphy.2022.964701.

[3] J. Portugali, "Cities, complexity and beyond," in *Handbook on Cities and Complexity*, Edward Elgar Publishing, 2021, pp. 13–27.

[4] E. Omodei, A. Bazzani, S. Rambaldi, P. Michieletto, and B. Giorgini, "The physics of the city: Pedestrians dynamics and crowding panic equation in venezia," *Quality & Quantity*, vol. 48, no. 1, pp. 347–373, Jan. 2014, ISSN: 1573-7845. DOI: 10.1007/s11135-012-9773-5. [Online]. Available: https://doi.org/10.1007/s11135-012-9773-5.

[5] L. Po, F. Rollo, C. Bachechi, and A. Corni, "From sensors data to urban traffic flow analysis," in *2019 IEEE International Smart Cities Conference (ISC2)*, 2019, pp. 478–485. DOI: 10.1109/ISC246665.2019.9071639.

[6] J. Lu, B. Li, H. Li, and A. Al-Barakani, "Expansion of city scale, traffic modes, traffic congestion, and air pollution," *Cities*, vol. 108, p. 102 974, 2021, ISSN: 0264-2751. DOI: https://doi.org/10.1016/j.cities.2020.102974. [Online]. Available: https://www.sciencedirect.com/science/article/pii/S0264275120313226.

[7] S. Jayasooriya and Y. Bandara, "Measuring the economic costs of traffic congestion," in *2017 Moratuwa Engineering Research Conference (MERCon)*, 2017, pp. 141–146. DOI: 10.1109/MERCon.2017.7980471.

[8] C. Yin, Z. Xiong, H. Chen, J. Wang, D. Cooper, and B. David, "A literature survey on smart cities," *Science China. Information Sciences*, vol. 58, no. 10, pp. 1–18, 2015.

[9] B. S. Kerner, "The physics of traffic," *Physics World*, vol. 12, no. 8, p. 25, Aug. 1999. DOI: 10.1088/2058-7058/12/8/30. [Online]. Available: https://dx.doi.org/10.1088/2058-7058/12/8/30.

[10] T. Nagatani, "The physics of traffic jams," *Reports on Progress in Physics*, vol. 65, no. 9, p. 1331, Aug. 2002. DOI: 10.1088/0034-4885/65/9/203. [Online]. Available: https://dx.doi.org/10.1088/0034-4885/65/9/203.

[11] M. J. Lighthill and G. B. Whitham, "On kinematic waves ii. a theory of traffic flow on long crowded roads," *Proceedings of the royal society of London. series a. mathematical and physical sciences*, vol. 229, no. 1178, pp. 317–345, 1955.

[12] D. C. Gazis, "The origins of traffic theory," *Operations Research*, vol. 50, no. 1, pp. 69–77, 2002.

[13] R. Herman and I. Prigogine, "A two-fluid approach to town traffic," *Science*, vol. 204, no. 4389, pp. 148–151, 1979.

[14] E. B. Lieberman, "Brief history of traffic simulation," *Traffic and Transportation Simulation*, vol. 17, 2014.

[15] L. Alessandretti, L. G. N. Orozco, M. Saberi, M. Szell, and F. Battiston, "Multimodal urban mobility and multilayer transport networks," *Environment and Planning B: Urban Analytics and City Science*, vol. 50, no. 8, pp. 2038–2070, 2023. DOI: 10.1177/23998083221108190. eprint: https://doi.org/10.1177/23998083221108190. [Online]. Available: https://doi.org/10.1177/23998083221108190.

[16] M. Batty, K. W. Axhausen, F. Giannotti, *et al.*, "Smart cities of the future," *The European Physical Journal Special Topics*, vol. 214, pp. 481–518, 2012.

[17] D. Cvetek, M. Muštra, N. Jelušić, and L. Tišljarić, "A survey of methods and technologies for congestion estimation based on multisource data fusion," *Applied Sciences*, vol. 11, no. 5, p. 2306, 2021.

[18] M. Bernas, B. Płaczek, W. Korski, P. Loska, J. Smyła, and P. Szymała, "A survey and comparison of low-cost sensing technologies for road traffic monitoring," *Sensors*, vol. 18, no. 10, 2018. DOI: 10.3390/s18103243. [Online]. Available: https://www.mdpi.com/1424-8220/18/10/3243.

[19] *Google maps*, https://maps.google.com, Accessed: 2024-06-10.

[20] J. Jain and G. Lyons, "The gift of travel time," *Journal of Transport Geography*, vol. 16, no. 2, pp. 81–89, 2008, ISSN: 0966-6923. DOI: https://doi.org/10.1016/j.jtrangeo.2007.05.001. [Online]. Available: https://www.sciencedirect.com/science/article/pii/S0966692307000531.

[21] A. M. Wahaballa, S. Hemdan, and F. Kurauchi, "Relationship between macroscopic fundamental diagram hysteresis and network-wide traffic conditions," *Transportation Research Procedia*, vol. 34, pp. 235–242, 2018, International Symposium of Transport Simulation (ISTS'18) and the International Workshop on Traffic Data Collection and its Standardization (IWTDCS'18)Emerging Transport Technologies for Next Generation Mobility, ISSN: 2352-1465. DOI: https://doi.org/10.1016/j.trpro.2018.11.037. [Online]. Available: https://www.sciencedirect.com/science/article/pii/S2352146518303260.

[22] T. VAN WOENSEL and N. VANDAELE, "Modeling traffic flows with queuing models: A review," *Asia-Pacific Journal of Operational Research*, vol. 24, no. 04, pp. 435–461, 2007. DOI: 10.1142/S0217595907001383. eprint: https://doi.org/10.1142/S0217595907001383. [Online]. Available: https://doi.org/10.1142/S0217595907001383.

[23] P. A. Lopez, M. Behrisch, L. Bieker-Walz, *et al.*, "Microscopic traffic simulation using sumo," in *The 21st IEEE International Conference on Intelligent Transportation Systems*, IEEE, 2018. [Online]. Available: https://elib.dlr.de/124092/.

[24] G. Gomes, *Open traffic models – a framework for hybrid simulation of transportation networks*, 2019. arXiv: 1908.04009 [cs.MS].

[25] E. Andreotti, A. Bazzani, S. Rambaldi, N. Guglielmi, and P. Freguglia, "Modeling traffic fluctuations and congestion on a road network," *Advances in Complex Systems*, vol. 18, no. 03n04, p. 1 550 009, 2015.

[26] G. Berselli, "Modelli di traffico per la formazione della congestione su una rete stradale," Ph.D. dissertation, 2022. [Online]. Available: http://amslaurea.unibo.it/26332/.

[27] G. Berselli and S. Balducci, *Framework for modelling dynamical complex systems.* https://github.com/sbaldu/DynamicalSystemFramework, 2024. [Online]. Available: https://github.com/sbaldu/DynamicalSystemFramework.

[28] E. W. Dijkstra, "A note on two problems in connexion with graphs," *Numerische mathematik*, vol. 1, no. 1, pp. 269–271, 1959.

[29] J. v. Brakel, *Robust peak detection algorithm using z-scores*, en, https://stackoverflow.com/questions/22583391/peak-signal-detection-in-realtime-timeseries-data, 2014. [Online]. Available: https://stackoverflow.com/questions/22583391/peak-signal-detection-in-realtime-timeseries-data/22640362#22640362 (visited on 04/12/2022).